12-15-2006

Analysis of Two Neighboring Miocene Paleo-Turbidite Systems in a Complex Deep-Water Environment: Implications for Biostratigraphic Techniques Used in Gulf of Mexico Petroleum Exploration Studies

Andrew Tipton
University of New Orleans

Analysis of Two Neighboring Miocene Paleo-Turbidite Systems in a Complex Deep-Water Environment: Implications for Biostratigraphic Techniques Used in Gulf of Mexico Petroleum Exploration Studies

A Thesis

Submitted to the Graduate Faculty of the
University of New Orleans
in partial fulfillment of the
requirements for the degree of

Master of Science
in
Geology

by

Andrew Bartholomew Steadman Tipton
B.S., University of Florida, 2000

December 2006

ACKNOWLEDGEMENTS

TABLE OF CONTENTS

LIST OF FIGURES

LIST OF TABLES

ABSTRACT

Biostratigraphic techniques are commonly used in shallow environments of the Gulf of Mexico basin for depositional history modeling in petroleum exploration applications. Extending these interpretations to deep-water settings, where the structural and depositional history is more complex, is problematic. A localized study area was used for a case-analysis of a typically complex deep-water study area. A dataset of seismic, well-log, and biostratigraphic information was used to: (a) assess accuracy of the biostratigraphic interpretations produced by Fillon (2005), (b) determine specific pitfalls of micropaleontology as a tool in this environment, and (c) provide guidelines for the application of biostratigraphic data in the deep-water. Results indicate that the previous depo-history modeling did not account for local complexity, thus lessening utility at the petroleum exploration scale. Future studies in this environment should account for sections transported down-dip, isolation of depocenters, autocyclic variability, and reduce reliance on the condensed section as a chronostratigraphic tool.

CHAPTER I

INTRODUCTION

Biostratigraphy is an essential tool in deciphering depositional history in the Gulf of Mexico basin. Many studies have appropriately applied biostratigraphy to the shallow neritic environments of the basin using techniques developed primarily for use in this setting. Applying the same biostratigraphic techniques and approaches to deeper-water (bathyal and abyssal) environments, with their complex depositional processes and convoluted structural history, is problematic. Variable sedimentation rates occur between intraslope minibasins, which are isolated by nature and have unique stratigraphic and structural characteristics. Allochthonous salt canopies further add to the structural complexity through stratal deformation and downslope displacement. These are two features (among others) of the deep-water bathyal and abyssal environments that do not exist on the shelf, and may significantly alter the applicability of biostratigraphic techniques that have been used previously in studies of shallower marine environments. This thesis will analyze a previous basin-wide biostratigraphic study for the accuracy and applicability of its results within the deep-water environment at the petroleum exploration scale. Exploration activity has been underway in the deep-water Gulf of Mexico for more than 15 years, and regional studies in the deep-water can benefit from a reexamination of the application of current shallow-water biostratigraphic approaches—within strata deposited beyond the shelf edge.

Study Area

The area of study is intended to provide a case analysis of two intra-slope minibasin fields and the biostratigraphic interpretations that can be made between them as an example of a complex deep-water setting. This deep-water study area contains the subsalt K-2 field and the

neighboring suprasalt Marco Polo field and minibasin (Figure 1). These fields are located in the

southeast portion of the Green Canyon federal leasing area, and are active hydrocarbon

producers. These fields were chosen for study because of their stratigraphic and structural

complexity, relevancy to petroleum exploration, and availability of publishable data. The fields

are separated by a distance of approximately 9 km. The deep-water Gulf of Mexico is an ideal

location for this study because: 1) intense exploration is currently underway in the basin, 2)

exploration is consistently being pushed basinward, and 3) its complex geology (e.g. Cenozoic

sea-level fluctuations, salt migration) makes it a good example of how multiple deep-water

processes can impact exploration studies.
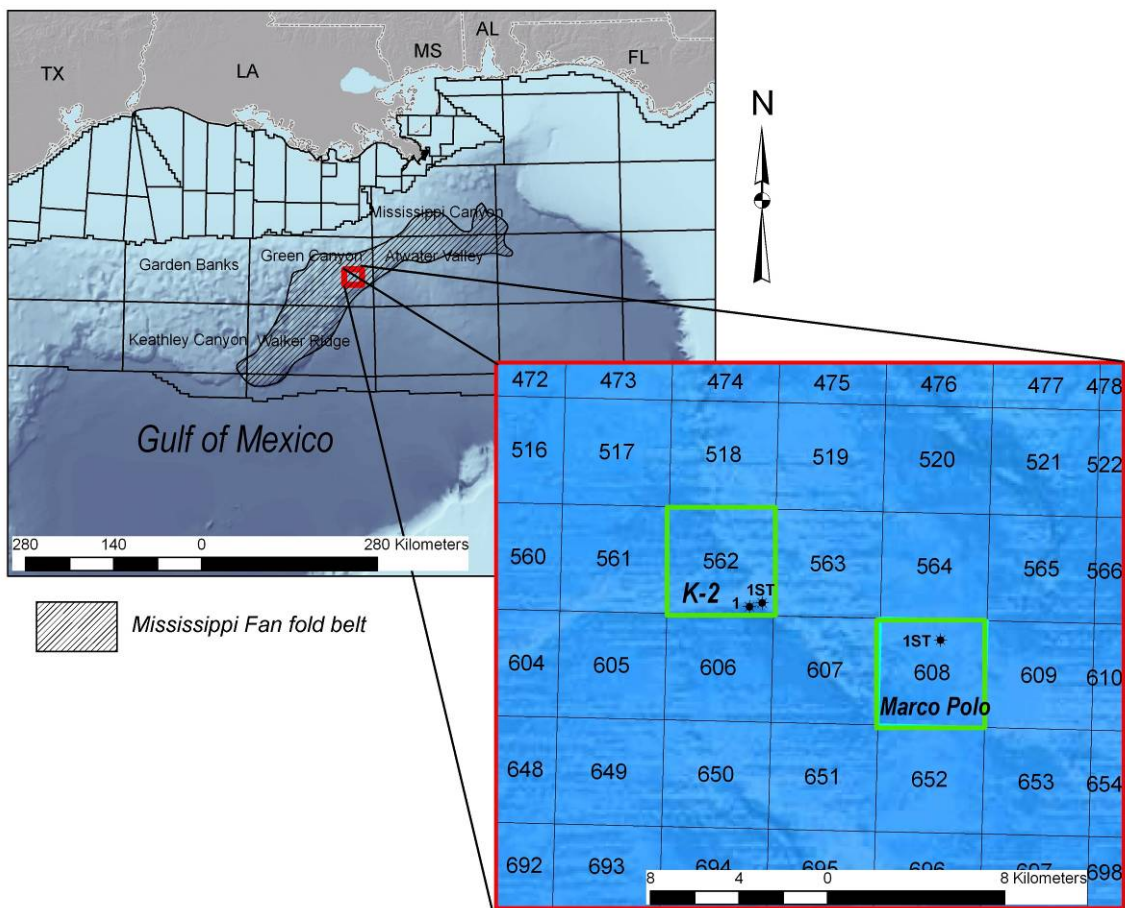
Figure 1—The study area includes the federal leasing blocks (GC562, GC608) where the K-2 and Marco Polo fields are located. Irregular sea-floor relief is a manifestation of salt-related features such as ponded minibasins. The Mississippi Fan fold belt province is shown in the hatched area on the large-scale map.

Depositional Systems

The geology of the study area is typical of the deep water environments of the Gulf of Mexico, inasmuch as the Cenozoic history of the study area dominantly reflects the interactions between halokinetics and cyclic turbidite deposition. On the basis of regional geology overviews, (e.g., Weimer, 1998; Slatt, 2006) facies tracts within the study area should contain all major architectural elements of turbidite systems, including: (a) erosional and leveed channels, (b) overbank deposits, (c) channel/fan transition zones, and (d) fan lobes (Figure 2). Chaotically stratified mass transport deposits (e.g. slump blocks), which may contain allochthonous shelf-edge facies associations, are potentially present in the study area.   In this study, a turbidite system is defined as a body of genetically related mass-flow and turbidity current facies and facies associations that were deposited in virtual stratigraphic continuity (Weimer et al., 1998). Turbidite systems are responsible for the transport of reservoir quality sands to the deep basin in the northern Gulf of Mexico (Reading and Richards, 1994). In fine-grained turbidite sytems, coarser fractions can be efficiently transported (up to several hundred kilometers or more) from the source (Mutti and Normark, 1991, Bouma, 2000). Source areas for turbidite flows vary with sea-level changes. During sea level high-stands, sediments sources can consist of prodelta and neritic deposits found near erosional turbiditic feeder channels. During sea-level lowstands the sediments from shallow marine and fluvial sources are immediately available from incised fluvial systems extending onto the shelf. The greatest contributions of sediment to turbidite systems during lowstands are from massive gravity failures of recently deposited shelf-edge deltas. The massive failures of these sediments are initiated by changes in intergranular pore pressures due to rapidly falling sea-level (Slatt, 2006). The three sand-rich architectural elements of turbidite systems that provide the greatest potential for hydrocarbon production are

channel deposits, proximal thinly bedded channel-levee overbank deposits, and basin floor sheet

fans. Basin floor fans typically provide the highest reservoir quality strata (Chapin et al., 1994).
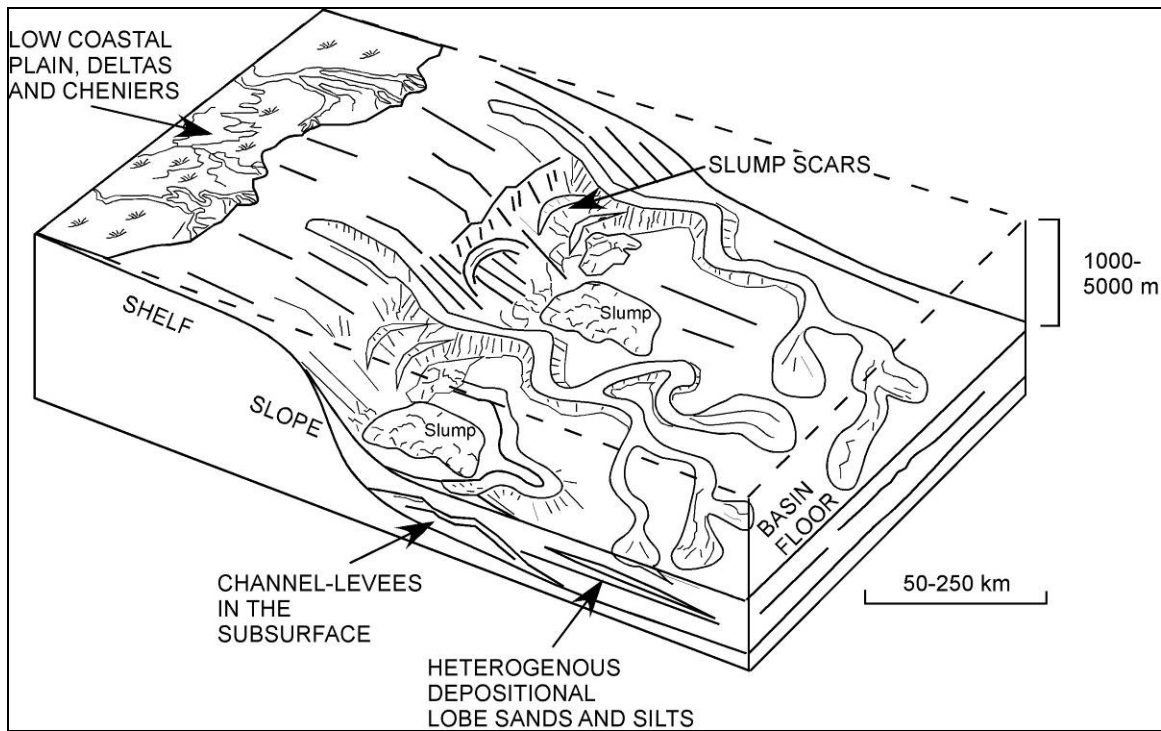
Figure 2—Depositional model of a typical fine-grained turbidite system such as in the Gulf of Mexico. Shelf-edge deltas during sea level lowstands are a significant source for sediments to the deep basin. It has been theorized that changes in pore pressures during rapid sea level fall can cause massive failures of young deltaic deposits perched at the shelf/slope transition (Slatt, 2006). Figure modified from Reading and Richards (1994).

Structural Features and Halokinetics

The study area lies within the Mississippi Fan fold belt province—a series of NE trending

folds near the toe of the continental slope. Deformation that created the fold belt was primarily

active from the Middle Miocene through Early Pliocene, and was caused by the basinward

sliding of rapidly deposited Cenozoic clastic sediments upon more unstable Mesozoic evaporites

(Morris and Weimer, 2004). Allochthonous salt bodies are extensive and well-developed within

the study area; where an apparently contiguous salt canopy is present throughout the study area.

Structure related to the fold belt occurs beneath the salt canopy, and as a consequence, is poorly

imaged in seismic surveys.
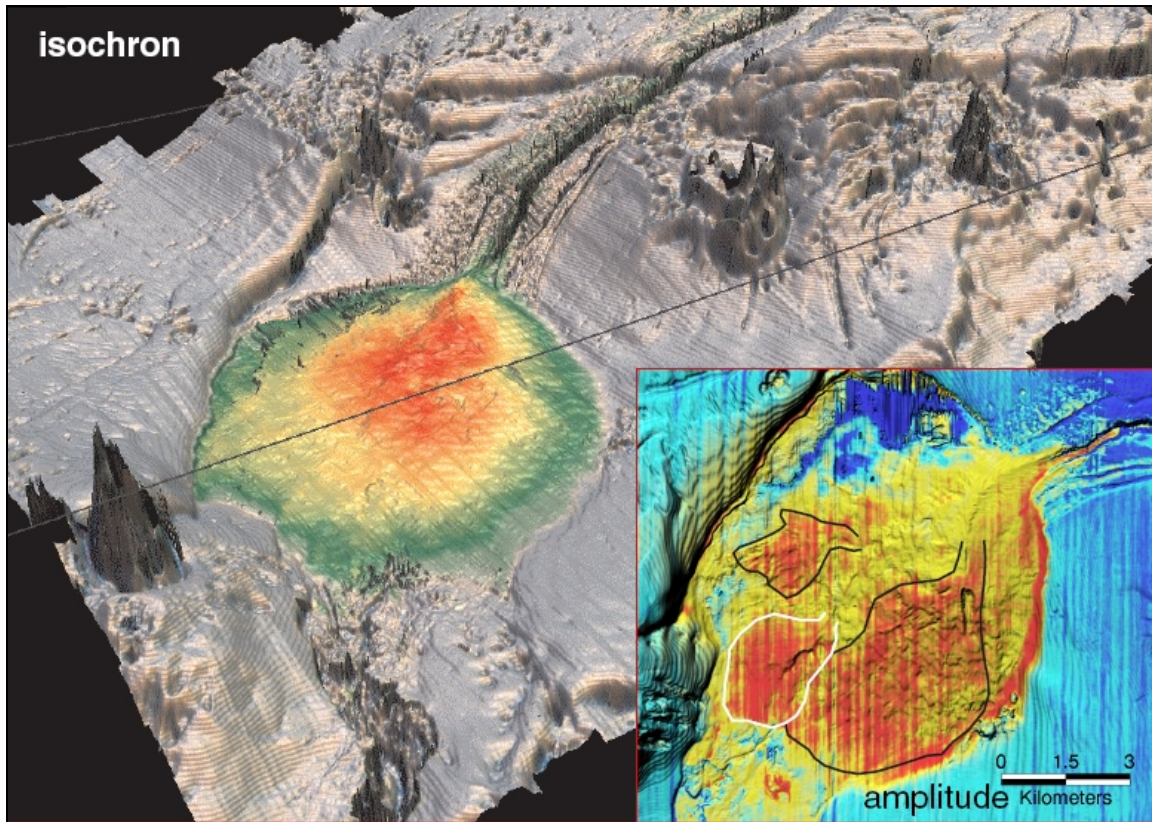
Figure 3—A sheet sand deposit within a ponded minibasin, offshore West Africa. Minibasin architecture is analogous to those located in the Gulf of Mexico. Hotter colors show areas of higher sand content, (Pirmez, 2000).

The interaction between salt movement and depositional processes is an important characteristic of turbidite systems within the Gulf of Mexico basin. The locations of deposits that are generated by turbiditic flows are controlled by bathymetric relief (Figure 3). Salt tectonics can have important effects on bathymetry in several ways: 1) Salt structures may create positive bathymetric relief due to diapir growth, or can create localized sinks (minibasins) as salt is evacuated and moves into diapers; 2) Downslope displacement of sediment by sliding on salt horizons creates extensional faults that may offset the sea floor, and create offsets which will serve to accelerate turbidite flows (Figure 4); 3) Counter regional faults (down thrown in the opposite direction to the regional bathymetric slope) often exist where thick salt is present, and can create obstacles to turbidite flows (Waltham and Davison, 2001). Minibasins are the primary

salt-created depocenters in the northern Gulf of Mexico slope, where sedimentation and halokinesis are contemporaneous processes that are continually interacting.
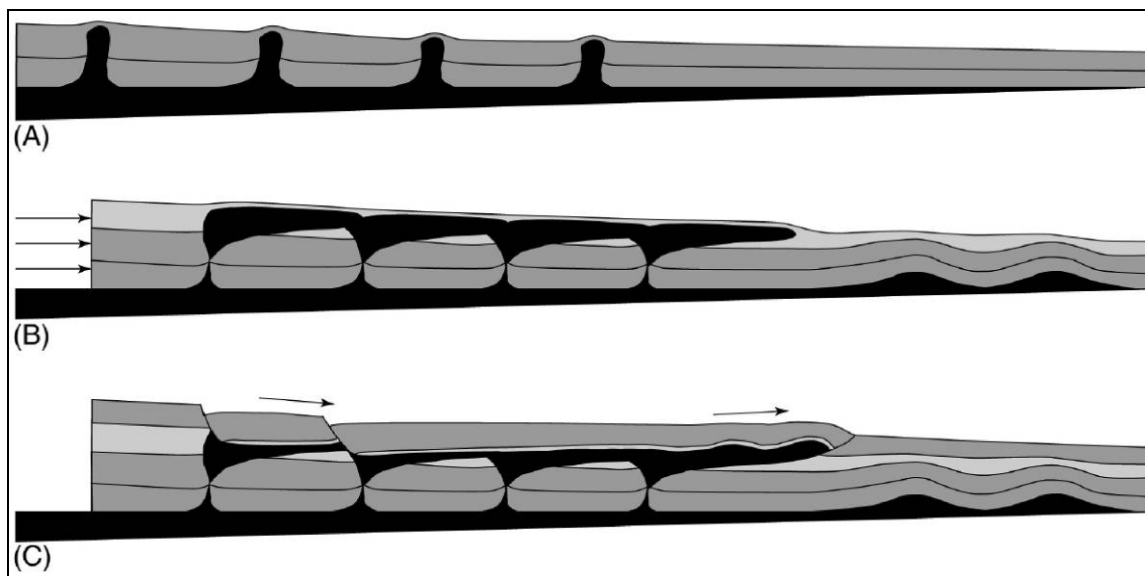
Figure 4—Role of allochthonous salt in accommodating gravitational failure of passive margins (reprinted from Rowan et al., 2001). (A) deep-water diapirs growing prior to contractional event; (B) lateral squeezing of diapirs during shortening, driving extrusion of salt tongues and canopy formation; (C) linked extension and contraction above the allochthonous detachment level.

Database

Paleontological reports containing micofossil event data were available for both the K-2 and Marco Polo fields from their respective operators—Ente Nazionale Idrocarburi (ENI) and Anadarko. Microfossil samples for wells within the fields were collected from rotary drill cuttings. The paleontological analysis for the K-2 field was performed by Applied Biostratigraphix of Houston, Texas, in October 1999. Paleontological analysis of the Marco Polo field was performed by Paleo-Data, Inc. of New Orleans, Louisiana, in July 2000. Detailed nannofossil reports, containing abundance and diversity curves, as well as sample-by-sample descriptions, were available for both fields. In addition, a detailed foraminiferal report with biofacies classifications was available for the Marco Polo field. A depth-migrated 3-D seismic volume was used to aid in stratigraphic correlations within the study area. The seismic volume was collected and processed for depth migration by WesternGeco. Due to the proprietary nature

6

of the seismic data, shot points and seismic traces could not be shown on any images. All images have been approved for publication by the seismic vendor. One well from each field was used in this study for reasons of simplicity of presentation and analysis. These wells—Conoco (CON) 562 #1 and Anadarko (ANA) 608 #1ST have very similar biostratigraphy with other wells drilled in their respective fields. Publicly available resistivity well logs for these wells were used to supplement the analysis.

The proprietary study *Gulf of Mexico Deposystems – 2005: Comprehensive Well Geohistory Datasets, Chronostratigraphy, and Maps* produced by Richard H. Fillon is a basin-wide biostratigraphic study that is available in its entirety. Fillon's study will be analyzed to fulfill the goals of this study—as it is an example of a study containing regional correlations that applies the same biostratigraphic techniques to both shallow and deep environments of the basin.

Objectives

Several recent studies of Gulf of Mexico depositional history have heavily incorporated biostratigraphy of deep water environments of the basin into their interpretations (Villamil, 1998; Fillon, 2005). Based on the uniqueness and complexity of the deep Gulf of Mexico basin, these studies may not have employed biostratigraphic techniques that are appropriate to the deep-water environment. There have been no previously published studies that specifically address the proper uses and limitations of biostratigraphic techniques in the deep-water Gulf of Mexico. This study provides:

1) An analysis of two deep-water fields utilizing multiple datasets that enables the opportunity to assess the accuracy of previous deep-water biostratigraphic depo-history models within this area. This analysis is focused on the study performed by Fillon (2005). An assessment of his regional-scale approach will be made from the knowledge

gained from the localized deep-water study area, as it is an example of the typical geologic complexity found on the continental slope.

2) A qualitative assessment of specific pitfalls of micropaleontology as a chronostratigraphic tool when used in the deep-water environment—focusing on the nature of deep-water deposition and retransportation, halokinetics, and the microfossil data collection process.

3) A general approach to a practical assessment of the potential reliability of biostratigraphic data that is obtained in various deep-water structural and stratigraphic settings. The intent is that these approaches and this information can be used by seismic stratigraphic interpreters.

CHAPTER II

BACKGROUND

Micropaleontology is a highly valuable resource for modeling the depositional history of Cenozoic clastic sedimentary basins. Coupled with stratigraphic models, micropaleontology can help to resolve the timing of glacio-eustatically controlled pulses of sedimentation and the identification of key depositional surfaces in the intensely studied Gulf of Mexico basin. Biostratigraphy enables major interpretive tools such as seismic data and well logs to be placed in a chronologic context. Seismic stratigraphic analysis requires the interpreter to have a basis for making chronostratigraphic correlations of reflector sets. In the Gulf of Mexico, biostratigraphy is the most practical and widely used method to place sediments in a near-absolute age context. Oxygen isotope analysis and radiometric dating of volcanic ash beds are two lesser utilized age dating techniques that have utility in specific instances.

Biostratigraphic events are routinely placed on well logs for correlation, and some log signatures can be directly correlated to biostratigraphic events (e.g. "hot shales" can support condensed section identification) (Crews et al., 1998). In the exploration industry the most commonly used bioevents are the *last appearance datum* (LAD) of individual taxa, with other lesser used zonations such as coiling changes in foraminifera and abundance peaks. The *first appearance datum* is usually only used when core data is available, because the rotary drilling process can mask the last downhole occurrence of a fossil by borehole sloughing. Because benthic foraminifera often inhabit discrete shelf and slope subenvironments—biofacies analysis can provide interpretations of paleo-water depth and environment. Detailed reservoir studies often incorporate high-resolution paleontology from conventional and side-wall cores to enhance stratigraphic and paleo-environmental modeling.

Biostratigraphic Techniques

Graphic Correlation

Biostratigraphers have developed sophisticated computer-based methods to bring full value to microfossil data. Foremost among these is the graphic correlation technique (Figure 5), which was first described by Shaw (1964), and has undergone multiple stages of refinement through time. Graphic correlation involves comparing a subject section containing paleontologic marker data with a complete reference section (or database of composite marker ages) containing the highest age resolution possible. By projecting the appearance of taxa from the reference section onto the subject section in an X-Y plot, a prediction can be made as to where those taxa should lie in the subject section, had they been present. Graphic correlation can also be used to find the locations of faults, condensed and expanded sections, and gaps in the subject section (Mann and Lane, 1995). In a related technique, sediment accumulation plots (also termed geohistory curves) are constructed for individual wells by placing borehole depth (preferably in *true vertical depth-TVD*) on the horizontal axis of an X-Y plot and absolute age of events from a composite standard reference section on the vertical axis (Figure 6). Biostratigraphic events are then plotted at their depth and age, and a line is drawn connecting them, tracing back to the origin. Accumulation rates (without any decompaction) can be interpreted from the slope of the connecting line. This technique assumes an accurate biostratigraphic interpretation and low structural dip. Where the slope of the line of correlation is near vertical, a condensed section is likely to be present (Villamil, 1998).
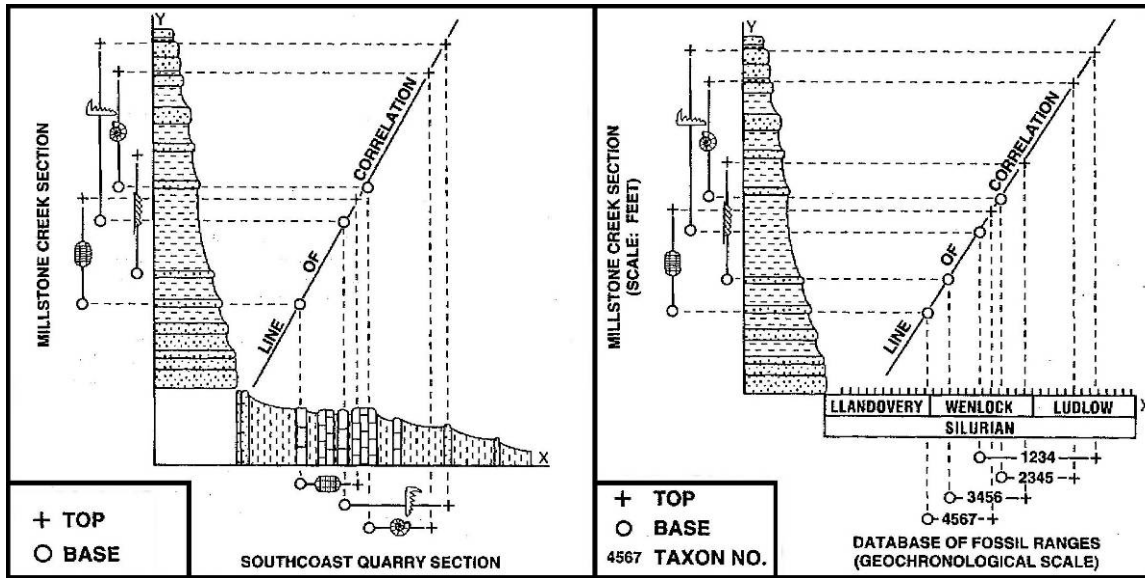
Figure 5—Example of graphic correlation. The diagram on the left compares two separate sections, whereas the right diagram compares a section to a composite fossil range database (reprinted from Mann and Lane, 1995).
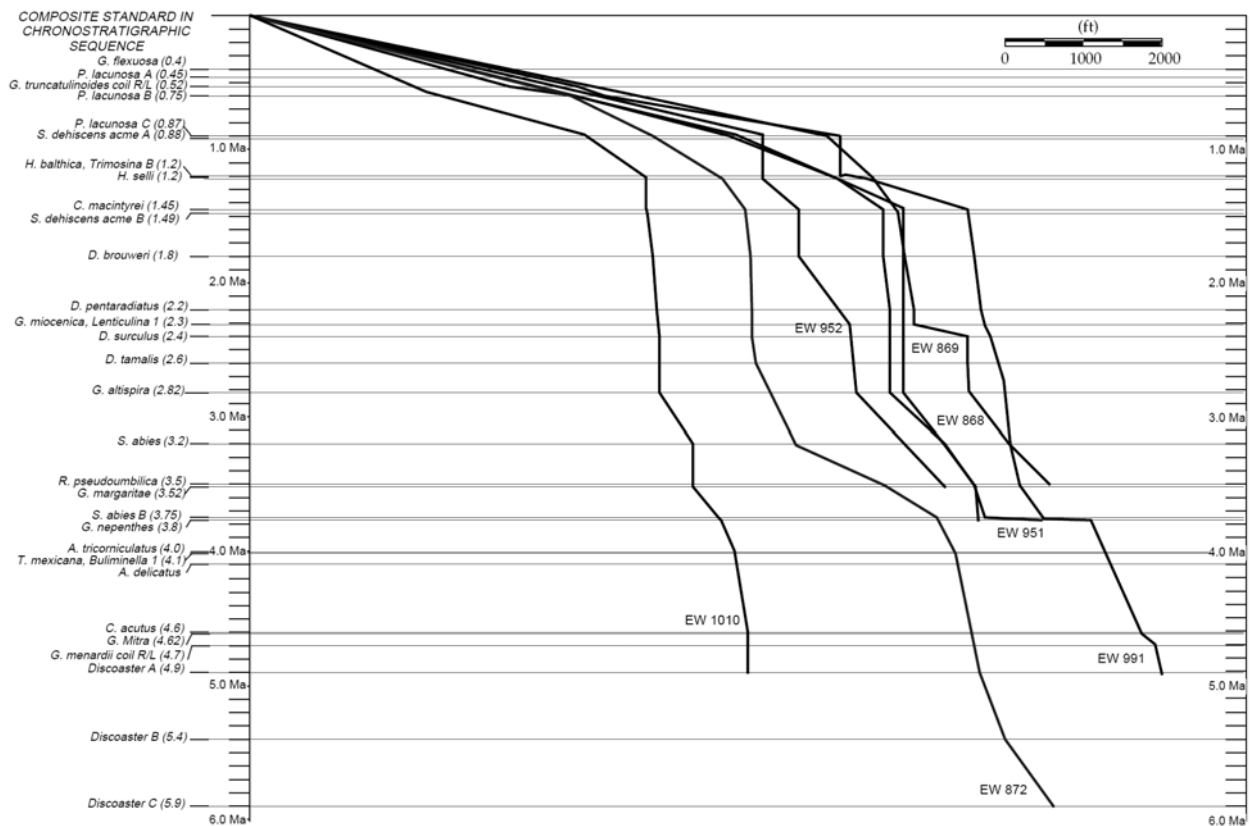
Figure 6—Example of sediment accumulation plots for multiple wells. The vertical axis shows ages of biostratigraphic events from a composite standard. The horizontal axis shows measured depth in feet (reprinted from Villamil et al, 1988).

Condensed Sections

When fossil data are used in a sequence stratigraphic framework their main utility lies in the recognition of condensed sections and maximum flooding surfaces (Emery and Myers, 1996). As defined by Loutit et al. (1988), a condensed interval is a thin marine stratigraphic unit consisting of pelagic and hemipelagic sediments characterized by very low sedimentation rates. Because they represent very long time intervals with low sedimentation rates, condensed sections are usually recognized by their abundant and diverse benthic and planktonic microfossil assemblages and authigenic mineralization. They can be recognized on well logs as "hot shales"—shales that have elevated gamma ray signatures due to the radioactivity present in minerals that can be deposited in the deep sea. Most "tops" or more correctly—*highest occurrences*—are picked within condensed intervals. This is due to the long periods of time elapsed within them and the assumption that fossils found within sandy facies are less reliable. Highest occurrences are most sharply defined with nannofossils because of environmental variability in the production of planktonic foraminifera (Shaffer, 1990). Along continental margins, transgressions in sea-level will cause sediment starved environments to shift up-slope as the primary depocenters are translated landward. Thus condensed sections can be correlated with maximum flooding surfaces (MFS) in paleo-shelf environments in a traditional sequence stratigraphic framework (Shaffer, 1990). In this context the condensed section can be interpreted as a chronostratigraphic event if the event is correlateable to a local or regional relative sea-level curve.

Biofacies Analysis

Biofacies analysis, which links the assemblages of benthic taxa to environmentally controlled factors, is primarily used as an indicator of paleobathymetry. It has also been

recognized that biofacies in the lower slope and abyssal settings are controlled by composition of bottom sediments, and thus can be termed litho-biofacies (Fillon, 2003). It has been noted that biofacies analysis is difficult, if not impossible, within turbidite deposits because of the potential for retransportation of benthic faunas from shallower environments. Because benthic biofacies are environmentally controlled, the highest occurrences of benthic faunas are difficult to establish as LADs in depositional settings that are not highly aggradational.

Previous Work

Fillon (2005) has produced a basin-wide study of the regional depositional history of the Gulf of Mexico for the Jurassic to latest Cenozoic. This study provides broad geological interpretations made solely from microfossil data, and thus was appropriate for review in this study. By utilizing a large database of well bore paleontology, he constructed sediment accumulation rate maps in 61 distinct biostratigraphically correlated sequences. These sequences were derived from a global sea-level cycle chart (Lawless et al., 1997). A proprietary computer-based statistical deconvolution method called *Stratrate* was used to resolve out-of-sequence tops and conflicting paleontological reports in each well (Fillon, personal comm.). *Stratrate* utilized graphic correlation to interpolate and insert the biostratigraphic sequence events that were not seen within wells. The true vertical thicknesses between events were then divided by the corresponding geologic time in each well, giving an accumulation rate in ft/Ma. A grid was created from approximately 12,000 offshore well control points using a kriging geostatistical method, and when contoured these data provided accumulation rate maps for each individual sequence. The microfossil data used in the Fillon (2005) study is publicly available and was obtained through the Minerals Management Service (MMS), and Paleo-Data, Inc. The K-2 and Marco Polo wells were not included in the Fillon (2005) database. The biostratigraphic

interpretations in the Fillon (2005) study were intended to be useful in exploration applications. For the purposes of this study it was therefore necessary to select a study area mapped in Fillon (2005), between control points, and of exploration significance. The methodologies used in Fillon's (2005) study are presented in Fillon and Lawless (1999) and Fillon and Lawless (2000).

To this author's knowledge, no complete studies have been published which specifically address the concerns of this thesis—namely, the concerns that exist in using common biostratigraphic techniques in the deep-water environment. Joyce et al. (1992) and Emery and Myers (1996) provide limited discussions of some of the specific uses of paleontology in the deep-water. Blake and Gary (1994) analyzes the use of biostratigraphy in an unrelated complex setting, the deep-water off of Trinidad.

CHAPTER III

METHODS

General Approach

Seismic imaging is valuable for structural imaging, reflector continuity correlations, direct hydrocarbon detection, and seismic facies interpretation among other uses. Well logs can provide hydrocarbon detection, lithology, pore pressures, petrophysical properties, and facies interpretations. When correctly applied, microfossils can provide the near-absolute age context essential to the previous two tools, as well as litho- and biofacies interpretations. Combining the assets of these three tools is common practice in the exploration industry, and is a practical way of assessing the reliability of the data contained in each individual method. This study utilized this integrated approach, as the modern seismic computing environment enables these datasets to be combined seamlessly. In addition to the following analytical techniques, a review of deep-water depositional process models and models of salt-sediment interaction was conducted for an in-depth discussion of the biostratigraphic implications of complex geological history of deep-water environments.

The analysis was conducted in three phases:

1. Seismic analysis, including—mapping relevant structural features, seismic facies and attributes.

2. Well log analysis—sand annotation, construction of structural cross-section, and turbidite facies classification from gamma ray patterns.

3. Biostratigraphic analysis and integration: Constructed series of maps that superimpose local geology (from phase 1) onto accumulation rate maps produced by Fillon (2005) in

order to compare with data obtained from the Marco Polo and K-2 wellbores. Sediment

accumulation rates were calculated for both the Marco Polo and K-2 fields.

Software Tools

The seismic interpretation suite used in the geologic analysis was Landmark Graphics

Corporation's OpenWorks. The seismic interpretation was performed in the SeisWorks 3D

module, and 3D visualization was performed with the EarthCube module. Well logs were

obtained through Lexco Data Sytems *Offshore Well and Lease Databases* (OWL). These logs

were digitized using NeuraLog, Inc.'s NeuraLog well log digitizing software and saved in the

Log ASCII Standard (LAS) format. The log curves were then imported into OpenWorks in order

to display them on seismic panels. A structural cross section was created in NeuraSection with

the digital well logs and biostratigraphic data. ArcView was used to view and edit accumulation

rate maps supplied in Fillon's (2005) dataset.

The nannofossil abundance data provided by the separate paleontological consultant

firms were supplied in different formats. Because of the importance of this data to condensed

section identification, it was important to convert the data into abundance logs of similar scales.

The K-2 report from Applied Biostratigraphix was supplied with total counts of faunal tests, and

the Marco Polo report from Paleo-Data, Inc. was supplied with an abundance histogram that was

normalized to a scale of 0 to 150. After consulting with A. Waterman (Paleo-Data), it was

determined that data from the K-2 report could be normalized to a similar scale as the Marco

Polo graph, because fossil abundance is a relative measurement. The resulting abundance log

curves were digitized and imported to OpenWorks.

3D Seismic Analysis

Seismic stratigraphy and seismic facies analysis was performed using the techniques outlined by Brown (2004), Prather et al. (1998) and to lesser extent Mitchum et al. (1977). Brown (2004) provides guidelines for analyzing seismic attributes such as RMS amplitude that can be used to interpret paleo-depositional systems through visual identification. Prather et al. (1998) provide a system (summarized in Table 3) that can relate seismic patterns and characteristics (e.g., undulation, mode of reflector termination) to broad classes of typical Gulf of Mexico depositional environments. An effort was made to identify any possible stratigraphic heterogeneity between the respective fields, and to make chronostratigraphic correlations of seismic reflector sets, because seismic reflectors can be interpreted as isochronous surfaces (Vail, 1977). Seismic facies analysis was necessary to support the goal of assessing the lithologic and stratigraphic continuity of the study area. The process involved the following tasks:

- Mapping of salt top and base throughout the study area.

- 3D visualization in EarthCube for broad structural perspectives.

- Establishing a well to seismic tie—No check shot surveys were available for either well, and no bulk density and sonic logs were available to construct synthetic seismograms. However, the salt canopy served as a datum to the nearby relevant biostratigraphic markers. Combined with the depth migration processing, this gave a reasonably accurate well to seismic tie to suit the purposes of this study.

- Horizon slice mapping—Reflectors with the potential to show depositional features within the Marco Polo minibasin were mapped for attribute extraction. K-2 was not mapped for this purpose because this approach is not applicable to subsalt imaging. This is due to dramatically reduced resolution and seismic energy beneath the salt. The

17

attribute that was extracted was RMS amplitude, which is the root mean square of

amplitudes within the windowed extraction interval. RMS amplitude is generally a good

method for identifying changes in lithology or hydrocarbons (Chen and Sidney, 1997). It

is often used to map depositional facies in the Gulf of Mexico, but must be performed at

relatively short two-way travel times (i.e. higher energy, higher resolution reflectors) that

are usually less than 2000 ms below the sea floor for any possible pattern recognition.

- Seismic facies from reflector characteristics—In deeper zones where resolution was

    lower, classifications of reflector styles were made to interpret potential depositional

    environments.

Log Analysis

Gamma ray log patterns were given general facies classifications based on the well log

patterns described by Mitchum et al. (1993), and Prather et al. (1998). In the depth ranges that

these wells penetrate, low gamma ray counts were interpreted as sandy zones, and were filled in

with yellow annotation behind the curve. Blocky "box car" type sand patterns were easily

identifiable as amalgamated sheet sands, although there exists some ambiguity in the

interpretation of log response patterns for distal sheet sands and proximal channel/levee facies.

Biostratigraphic Analysis

Because this study deals with correlations between the respective fields, only

biostratigraphic events that share a common time interval in both wells were involved in

correlation analysis. There were six correlatable biostratigraphic events that were common to

both wells. The LADs of the observed biostratigraphic markers were obtained from the widely

used Paleo-Data, Inc. Biostratigraphic Chart for the Neogene. Five of these events correspond to

either defined sequence events or are age-equivalent to sequence events used in Fillon's (2005)

study, from sequences 16 through 21 (Lawless et al., 1997). Two complete sequences (16 and 17) and one composite interval (18 to 20) were present in the wells. The stratigraphic thicknesses of these sequence intervals and their accumulation rates were calculated for both wells. True stratigraphic thickness of each interval was calculated because significantly dipping reflectors were observed in seismic views. This was performed by constructing a dip amplitude map of a horizon near the relevant picks and estimating an average dip near the well bore, then multiplying the cosine of the dip by the true vertical depth of the interval. The interval thicknesses used in calculating accumulation rate were not corrected for compaction, so the calculated value was taken as a minimum accumulation rate (Tables 1 and 2).

Fillon's (2005) accumulation rate maps were imported into ArcView, and polygons of approximate suprasalt minibasin extents (with likely older Miocene sections) within the study area were superimposed onto sequences 16, 17, 18, and 19. The minibasin polygons were created from top of salt structure maps.

EVENT NAME	Fillon (2005) Seq. No.or Equivalency	Measured Depth (ft)	TVD (ft)	LAD (Ma)	Seq. Interval thickness (ft)	Apparent Dip (deg)	Seq. TST (ft)	Seq. Accum. Rate (ft/Ma)
Discoaster bollii	16	21120	21080	9.1	100	25	91	303
Discoaster hamatus	17	21220	21180	9.4	578	25	526	1052
Catinaster coalitus	na	21800	21758	9.9	na	25	na	na
*Coccolithus miopelagicus**	18*	22480	22436	11	1258	25	1140	712
Discoaster sanmiguelensis	~20	22720	22674	12.82	na	25	na	na
Cyclicargolithus floridanus	na	22960	22913	13.45	na	na	na	na

Table 1—Correlatable biostratigraphic events of CON 562 #1, and accumulation rate calculations. TVD=true vertical depth, LAD=last appearance datum, TST=true stratigraphic thickness. *Because a sequence 19 event was not available and sequence 20 was, a composite accumulation rate was calculated for sequences 18 and 19.

EVENT NAME	Fillon (2005) Seq. No. or Equivalency	Measured Depth (ft)	TVD (ft)	LAD (Ma)	Seq. Interval Thickness (ft)	Apparent Dip (deg)	Seq. TST (ft)	Seq. Accum. Rate (ft/Ma)
Discoaster bollii	16	16030	14785	9.1	251	20	236	787
Discoaster hamatus	17	16330	15036	9.4	210	20	197	394
Catinater coalitus	na	16580	15246	9.9	na	20	na	na
*Coccolithus miopelagicus**	18*	17780	16291	11	1341	20	1260	787
Discoaster sanmiguelensis	~20	18110	16587	12.82	na	20	na	na
Cyclicargolithus floridanus	na	18320	16777	13.45	na	na	na	na

Table 2—Correlatable biostratigraphic events of ANA 608 #1ST, and accumulation rate calculations. *Because a sequence 19 event was not available and sequence 20 was, a composite accumulation rate was calculated for sequences 18 and 19.

CHAPTER IV

RESULTS

Relevant Structure

The 3-D visualization and mapping of the study area revealed a contiguous salt canopy within the study area. No evidence of rooting to the source (Jurassic Louann salt) was visible within the study area or data, and therefore no salt welds were apparent. Figures 7 through 10 provide 3D overview perspectives of the study area.

K-2 Field

CON 562 #1 enters the salt canopy at 11,800 ft and exits at 21,100 ft. This well targeted dipping high amplitude reflections against a subsalt trap present as a locally enclosed high in the salt canopy (see Figures 7, 10, and 11). The apparent structural deformation observed below the salt is likely related to contractional folding within the Mississippi Fan fold belt province.

Marco Polo Field

The extents of the Marco Polo minibasin are visible in Figure 13. ANA 608 #1ST was drilled on the southern end of the Marco Polo minibasin, and the final depth of the well lies just above the salt canopy. This well was drilled through a synformal structural trap caused by failed diapiric growth of salt beneath (Figures 12 and 14). The failed diapir was recognized from a local salt high below the synform, and an erosional unconformity between stratigraphic packages A and C (Figure 17). Reflectors within the Marco Polo minibasin dip to the northwest. Seismic facies analysis revealed that sediment influx into the minibasin may have come from the northwest (Figure 18). Therefore, the observed structural dip is in the opposite direction of expected depositional dip, and post-depositional rotation was caused by either of the following:

(a) inflation of the underlying failed salt diaper, (b) differential inflation of the surrounding massive salt body on the southern boundary of the minibasin.
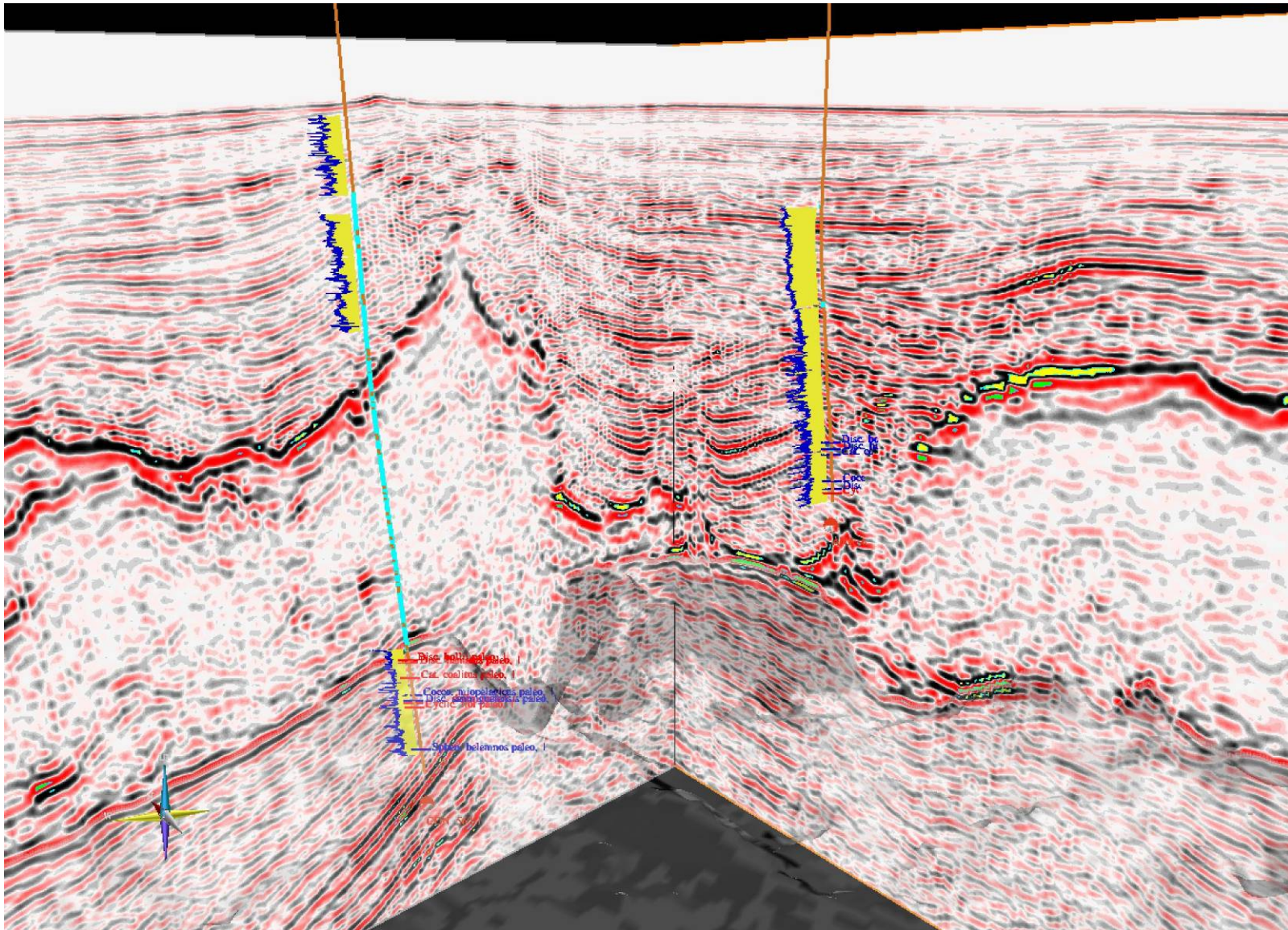
Figure 7—3D visualization of study area, perspective view looking due north (see 3D direction indicator in lower left corner, red arrow-north, light blue arrow-up).   Base of salt horizon is shown as a semitransparent shaded surface in the foreground. Vertical seismic panels are normal to each other in all subsequent 3D perspective images.
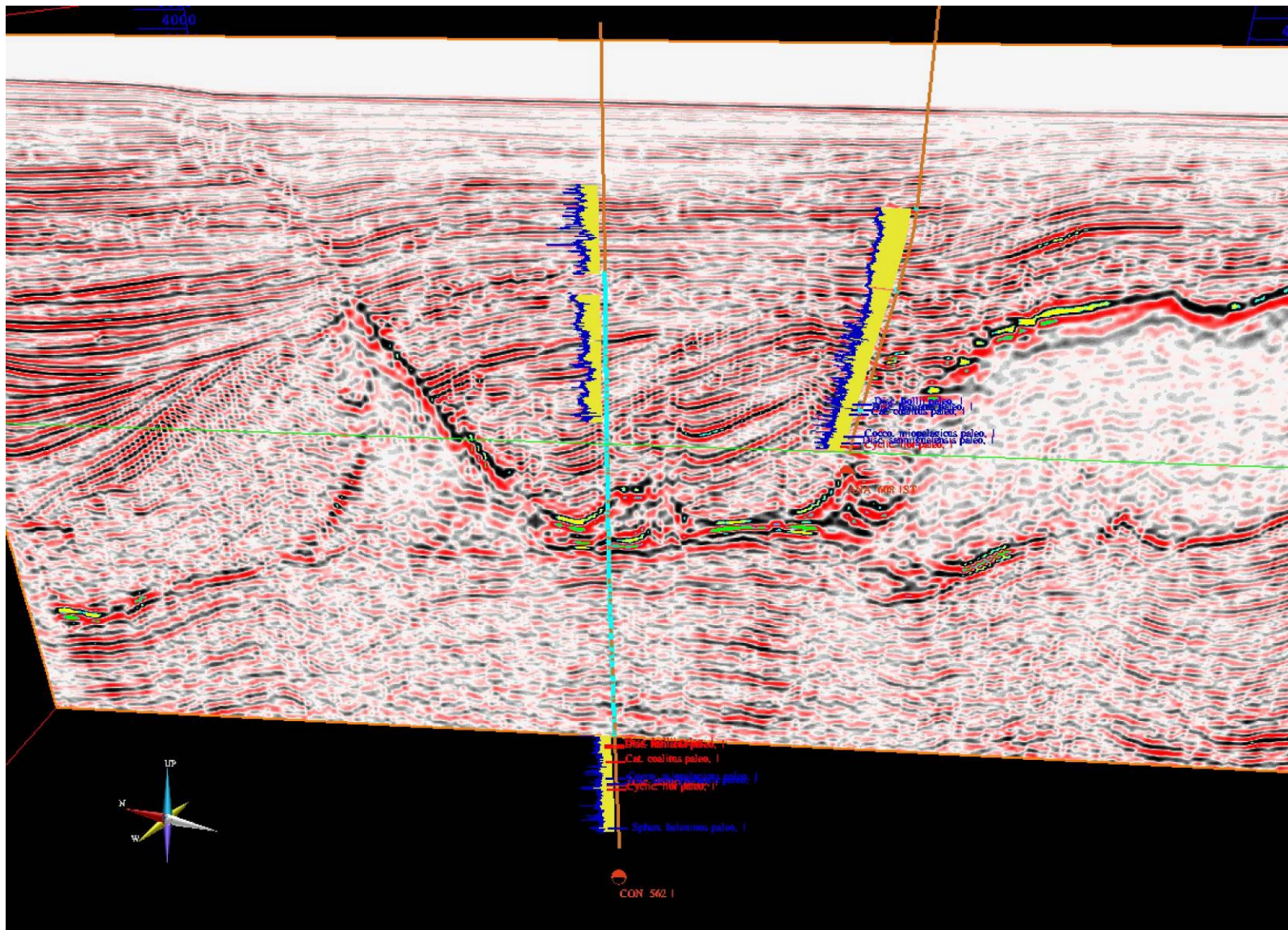
Figure 8—3D perspective view looking to the northeast. Salt is seen in areas bounded by strong reflectors, with chaotic and low amplitude internal reflections.
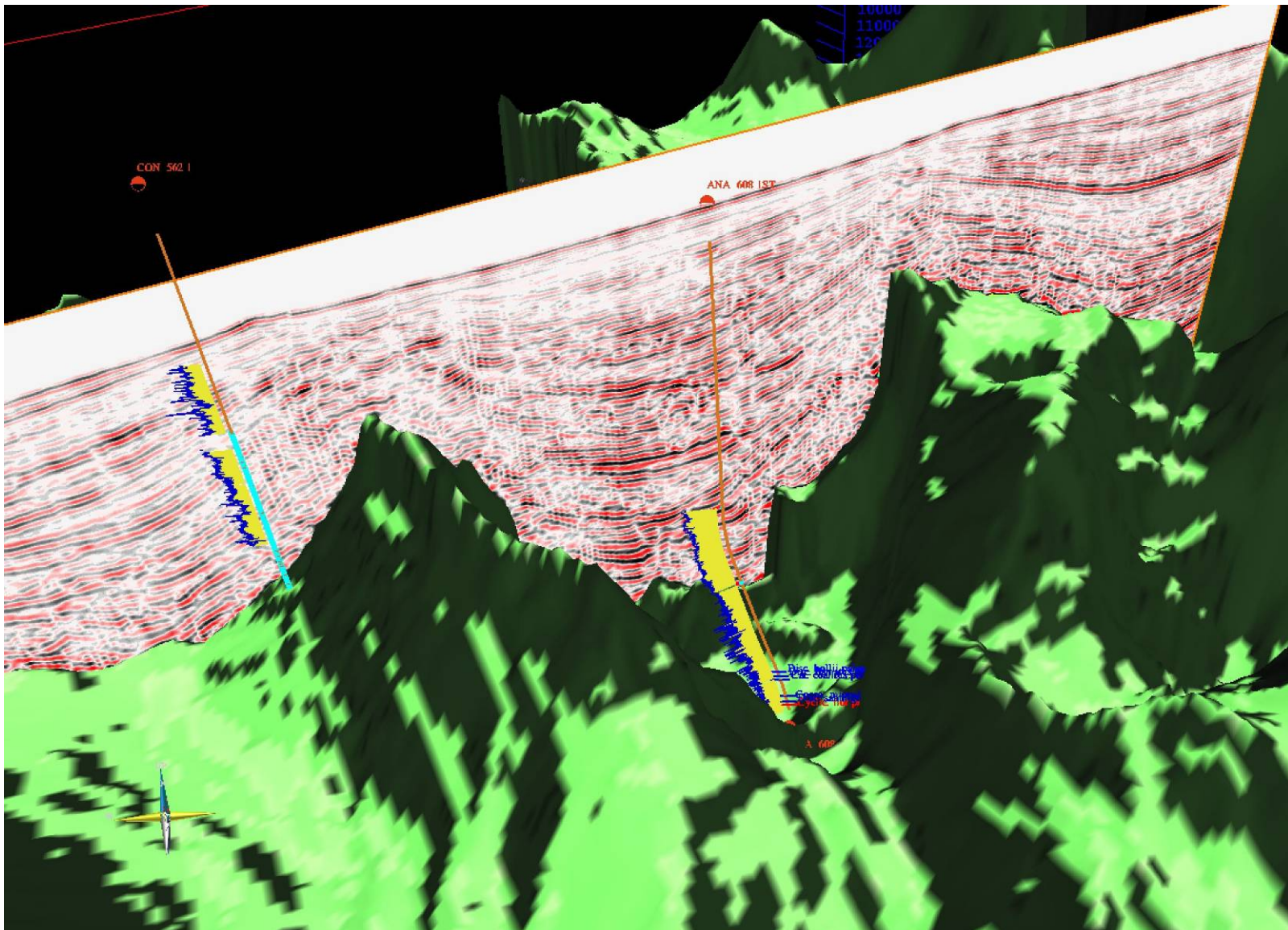
Figure 9—3D perspective view looking down and to the north, with the top of salt displayed as the green surface.
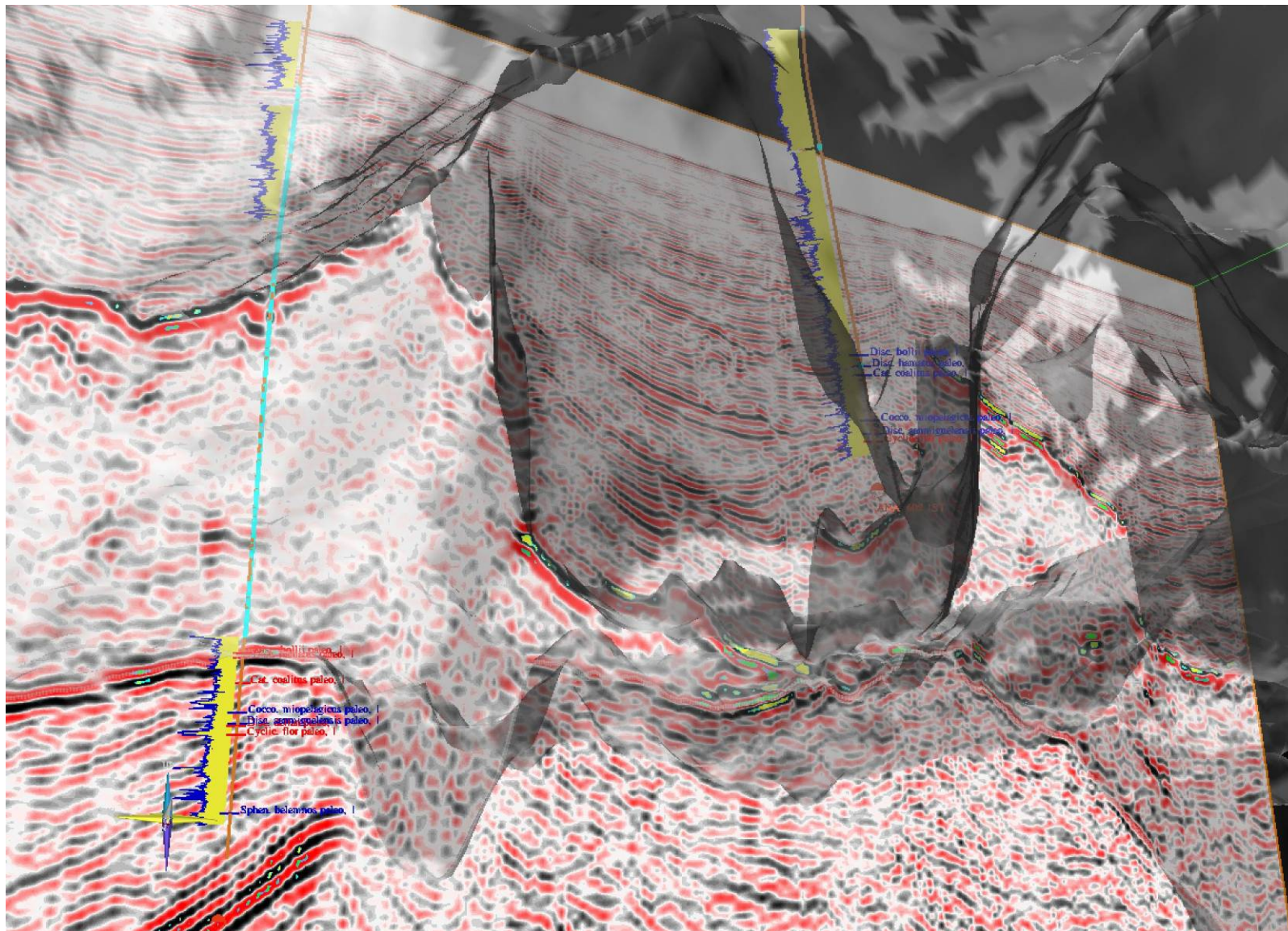
Figure 10—3D perspective view looking up and to the north from below the salt canopy. The base of salt and top of salt are visible as the upper and lower semitransparent surfaces, respectively.
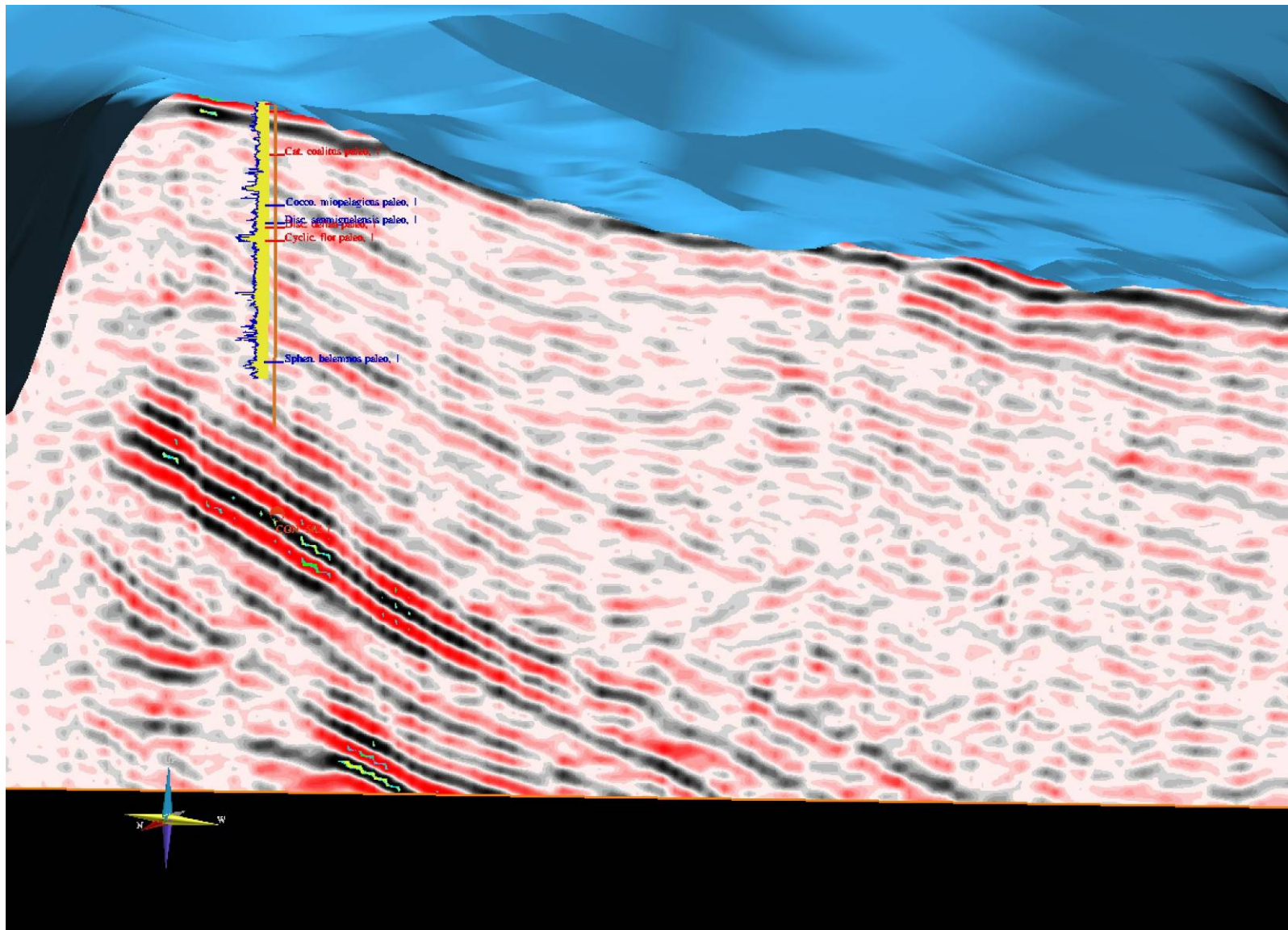
Figure 11—3D perspective view looking to the southwest at the subsalt portion of the K-2 well, showing the dipping structural trap. High amplitude reflections just below the final depth of the wellbore likely indicate the presence of Oligocene chalk.
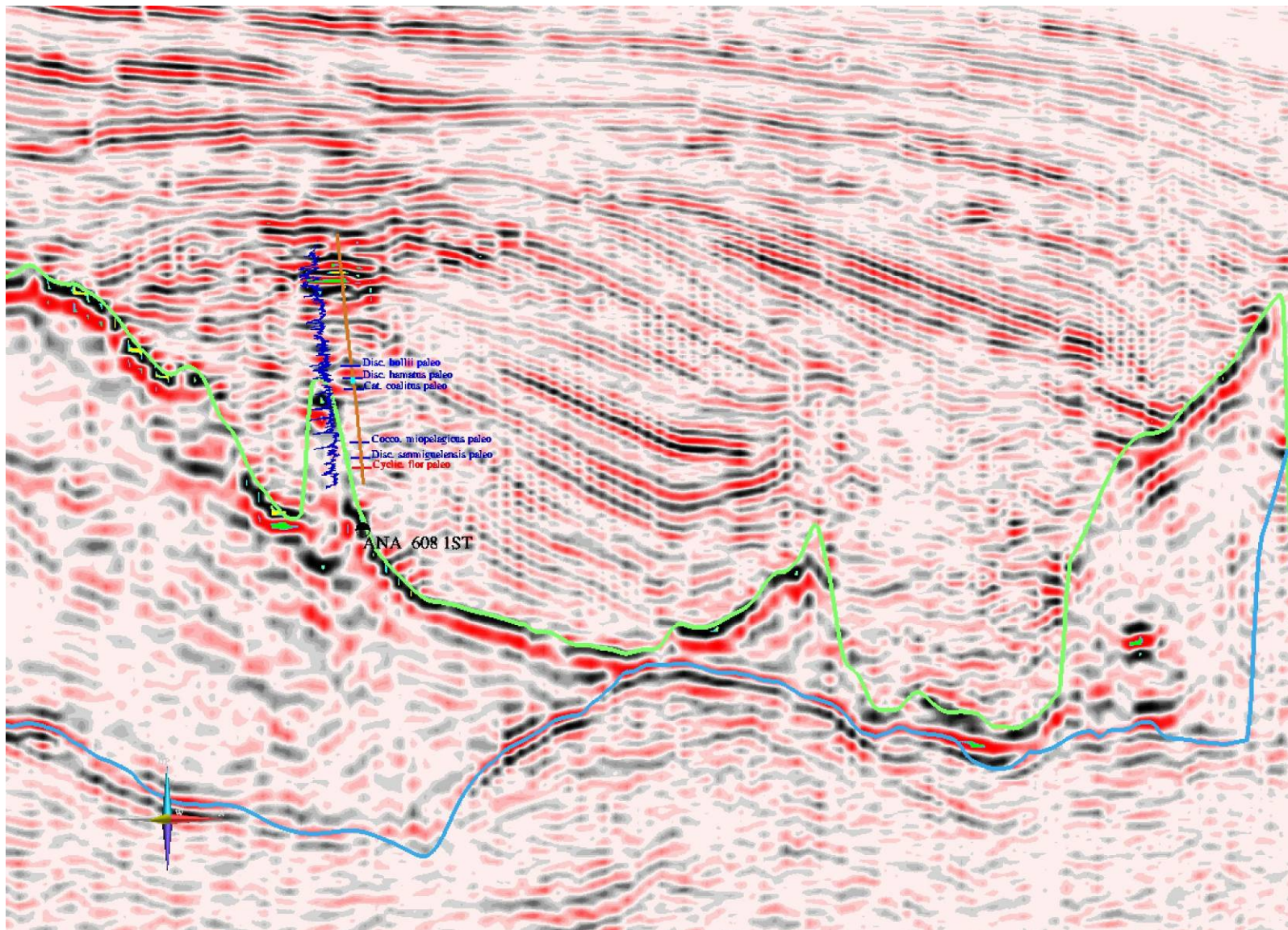
Figure 12—3D perspective view of the lower portion of the well bore in the Marco Polo field. The well bore disappears behind the vertical seismic panel because the well is deviated. Green and blue horizons indicate the top and base of salt, respectively.
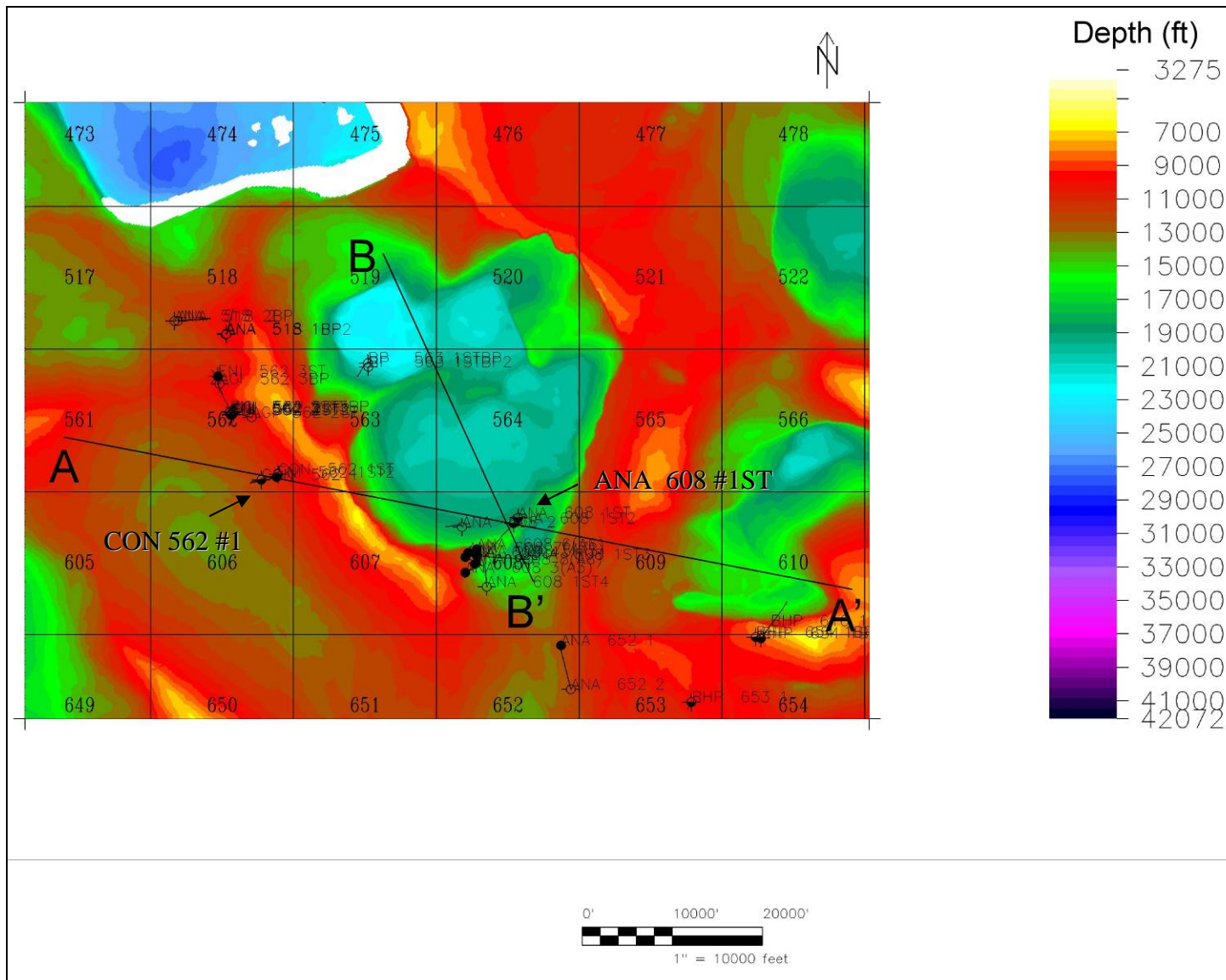
Figure 13—Depth structure map showing the top of salt, hotter colors are shallower and cooler colors are deeper. Sections A-A' and B-B' correspond to figures 14 and 17.
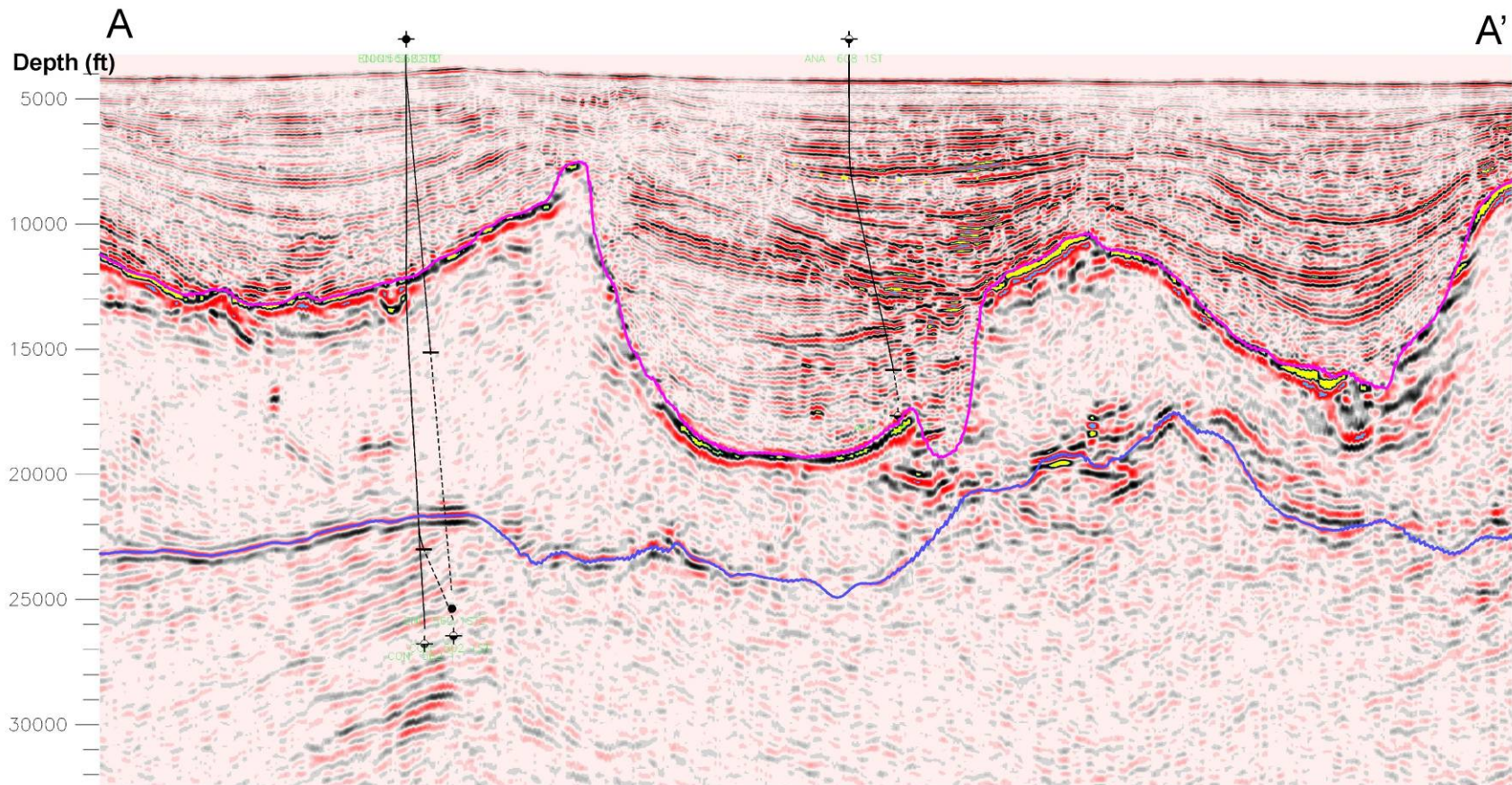
Figure 14—This seismic section is a direct tie from the K-2 field to Marco Polo field. Top and base of salt are shown as the pink and blue horizons, respectively. Location of section AA' is shown in map view in figure 13.

Stratigraphy

Six biostratigraphic markers are common to both wells; all markers are calcareous

nannoplankton LADs. These nannoplankton markers are listed below:

- *Discoaster bollii*-9.1Ma, Late Miocene

- *Discoaster hamatus*-9.4 Ma, Late Miocene

- *Catinaster coalitus*-9.9 Ma Late Miocene

- *Coccolithus miopelagicus*-11.0 Ma Middle Miocene

- *Discoaster sanmiguelensis*-12.82 Ma Middle Miocene

- *Cyclicargolithus floridanus*-13.45 Ma Middle Miocene

The nannofossil abundance curves show no correlateable peaks between the two wells

(Figure 15). Figure 15 shows a structural cross-section between the fields. At the K-2 well,

the base of salt was seen at 21,080 ft TVD, where the highest occurrence of *Discoaster bollii*

was picked. The well terminates in Lower Miocene section. *Discoaster bollii*, the highest

common event in the Marco Polo well, was picked at 14,785 ft TVD. These age-correlated

events are separated by 6,295 vertical ft and a horizontal distance of 28,764 ft. As illustrated

by the cross-section, all age correlated sections in Marco Polo are structurally high relative to

those at K-2 (Figure 15). The sediment accumulation plots (Figure 16) reveal that zones near

the boreholes show different accumulation rate histories between the fields, however the

rates for each interval are within one order of magnitude. A possible condensed interval is

present between *Coccolithus miopelagicus* and *Discoaster sanmiguelensis* in both wells

(Figure 16). The calculated accumulation rates for the sequence interval 18-20 were

approximately the same at both fields, at 712 and 787 ft/Ma for the K-2 and Marco Polo,

respectively.
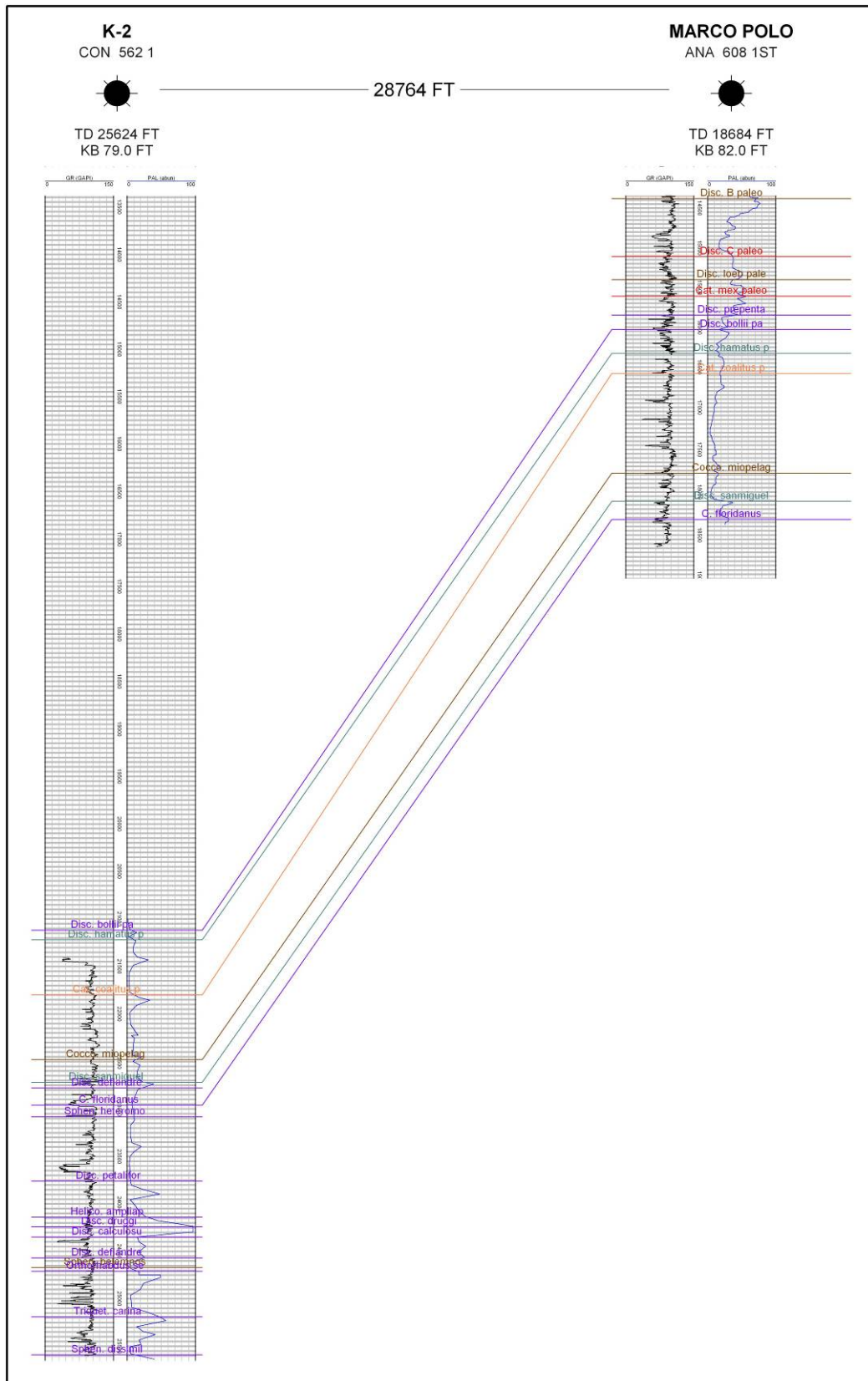
Figure 15—Structural cross-section with correlations based solely on common microfossils. Gamma ray curve is in the left track, nannoplankton abundance curve is in the right track.
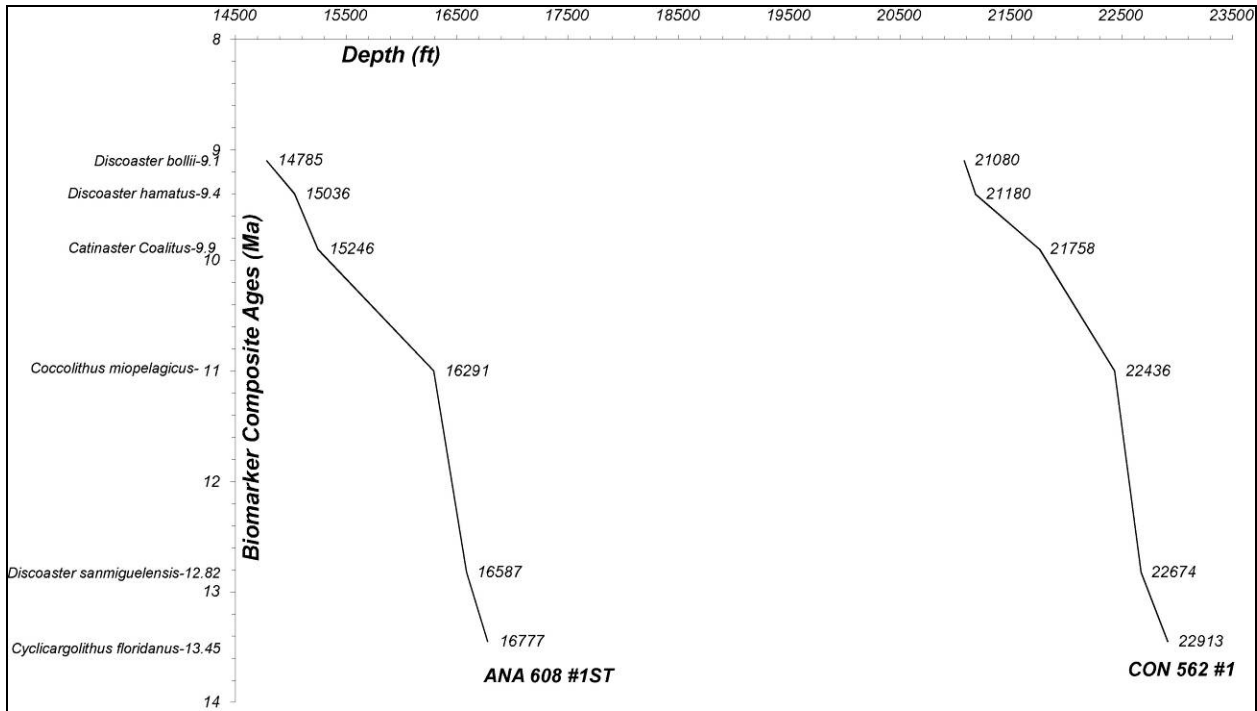
Figure 16—Sediment accumulation plots for the respective wells in their age equivalent intervals. A possible condensed interval lies between *Coccolithus miopelagicus* and *Discoaster sanmiguelensis* in both wells. Biomarker ages are from the Paleo-Data, Inc. biostratigraphic chart.

The 3D visualization revealed a salt canopy that was contiguous. Because the canopy is unbroken, and the two fields are separated by it (Figure 14), there were no correlateable depositional reflectors between the age-equivalent packages in either well. The likeliest explanation for the presence of this seemingly incongruous time discontinuity is that the suprasalt Marco Polo section has been rafted downslope from an up-dip location, through gravity sliding of the allochthonous salt canopy as described in halokinetic models by Rowan et al. (2001) and others (Figure 4). Downslope transportation of the entire minibasin may have contributed to the stratal rotation that was observed.

Seismic and Well Log Facies

Seismic reflectors within the Marco Polo minibasin were separated into five separate packages, based on the reflector characteristics and unconformities. Table 3 provides a summary of the classification criteria. The stratigraphically lowest package—labeled (A) in Figure 17, exhibited high amplitude reflections that converged by baselap at the basin margins, and was interpreted as basin floor or slope fan facies assemblages. Package (B) contained comparatively low amplitude reflections that were terminated by thinning. This is indicative of fine-grained assemblages such as overbank deposits, and was not interpreted as hemipelagic drape due to lack of reflector continuity. Package (C) exhibited high amplitude chaotic reflections with erosional basal contacts that resulted from turbiditic feeder channel systems and channel sands. Package (D) exhibited high amplitude reflections that were terminated by baselap. The high amplitude reflections indicate basin floor or slope fans with possibly thick amalgamated sands. Package (E) exhibited highly chaotic, high amplitude reflections, and was interpreted as turbiditic feeder channels and associated sands.

Seven RMS amplitude extractions were performed on horizons at different levels within the Marco Polo minibasin. In only the shallowest attempt (approximately 8900 ft) were any patterns recognized. Turbidite feeder channels and proximal fan lobes were observed (Figure 18), supporting the previous interpretation of package (E).The deepest six attempts were unable to achieve any viable imaging presumably due to the many small faults that are present within the basin, and the diminished seismic signal with depth.

No seismic facies were able to be described at the K-2 field, as seismic energy was greatly diminished below the salt. High amplitude reflections below the final depth of the well likely indicate the top the extensive Oligocene chalk that is present in this area of the basin.

Though seismic facies were not present, well log facies analysis of K-2 (Figure 19) revealed blocky gamma ray response patterns in several intervals that are typical of basin floor fans (Mitchum et al., 1993, Prather et al., 1998), separated by thick low-resistivity shaly intervals. The gamma log at the Marco Polo well (Figure 20) showed an overall sand poor response in the Upper to Middle Miocene sections. Shales showed sawtooth patterns with slightly low gamma counts (sandier) that are typical of slope bypass facies. Sands had an overall high gamma response (shalier) and were relatively thin. This is consistent with slope fan and slope bypass facies, which are the interpreted depositional environments for this interval.

Facies	Reflectivity	Reflector Geometry	Rock Types	Environment	Comments
Chaotic with rotated blocks	Low to high	Chaotic with rotated blocks, faults sole out at base	Variable	Slope failures, slumps	Lithology dependent on precursor material incorporated into slump; recognition is heavily dependent on line orientation
Chaotic, high reflectivitiy	Variable to high	Chaotic or wavy; discontinuous; erosional basal contact common	Discontinuous channelized sands with interchannel mudstone	Turbidite feeder channel system, amalgamated channel sands	Rapid facies changes; subdivision of a and b packages is heavily dependent on line orientation; lithology dependent on precursor mater incorporated into the slide
Chaotic; low reflectivity	Low	Transparent, chaotic or wavy; locally mounded and onlapped; erosional basal contact	Mudstone with highly discontinuous claystone and siltstone beds	Mass flow units of variable lithology	
Convergent by baselap, high reflectivity	Variable to high	Convergent by baselap at paleobasin margins; variable to high reflector continuity	Interbedded sand, mudstone, and claystone	Basin-floor and slope submarine-fan complexes with both sand sheets and leveed channels	Multiple baselapping seismic events implies bottom-hugging gravity flow deposition in confined setting usually associated with a presence of sandstones; differentiation based on reflectivity may depend on line orientation and depth. Low reflectivity results from seismic packages composed of rocks with small impedance contrasts, which implies uniform lithology; shale compaction due to burial age,
Convergent by baselap, low reflectivity	Low	Convergent by baselap at paleobasin margins; variable to high reflector continuity	Interbedded sand, mudstone, and claystone	Probably ponded mass flows or sand-rich submarine fans	
Convergent by thinning, high reflectivity	Variable to high	Convergent by thinning at paleobasin margin; variable reflector continuity	Thin bedded sands within claystone and mudstone	Leveed-channel, overbank, and distal thin-bedded turbidites with fine-grained suspension fallout and hemipelagic drape on slope	
Convergent by thinning, low reflectivity	Low	Convergent by thinning at paleobasin margin; high reflector continuity	Few thin-beeded sands with mudstones and claystones	Fine-grained suspension fallout, muddy or overbank turbidites, and hemipelagic drape on slope	or low seismic frequency content
Draping high impedance	--	Draping, generally continuous, single, high-acoustic-impedance loop or doublet	Predominantly claystone and mudstone with some marls and foram-rich claystones	Muddy turbidites to condensed section	Convergences may occur at a scale larger than single instraslope basin; therefore, it may be closely related to convergent thinning facies; it also may represent condensed zones between stacked layers of convergent by baselap
Draping low impedance	--	Very continuous, draping, single low-acoustic impedance loop of uniform thickness	Claystone, forma-rich claystone, marl, or chalk	Deepest basin, condensed section and pelagic-hemipelagic drape	

Table 3—Seismic facies classification chart based on reflector characteristics and geometry (from Prather et al., 1998).
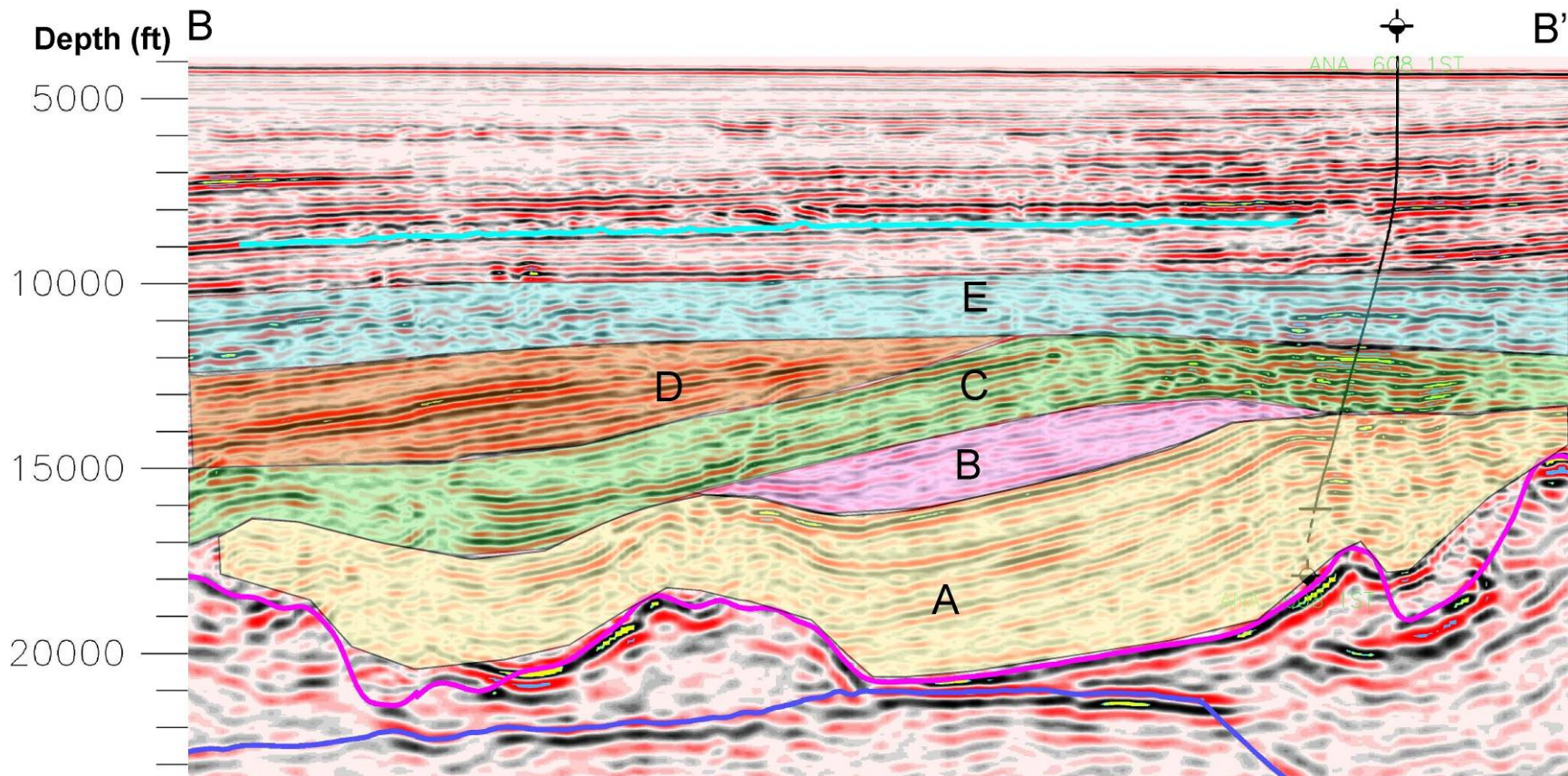
Figure 17—Strike perspective section showing facies classifications. Seismic facies were distinguished utilizing the techniques of Prather et al. (1998), and five generalized zones were developed. The upper light blue horizon was extracted for RMS amplitude attributes, shown in figure 18. Environmental interpretations—Package A: Basin floor or slope fan facies assemblages. Package B: Sand poor fine-grained fan assemblages including levee overbank deposits. Package C: Turbidite feeder channel system. Package D: Ponded mass flows, with possible thick amalgamated sands. Package E: Turbidite feeder channel system.

Figure 18—RMS amplitude extraction from the upper light blue horizon in Fig. 17, which is at a depth of approximately 8900 ft. The left lobe is interpreted as a channel/fan transition zone due to the dendritic channel patterns emanating from the channel source. The sinuous channel on the right bifurcates into an area that is possibly a channel/lobe transition zone. These systems are Pleistocene on the basis of available biostratigraphic data.
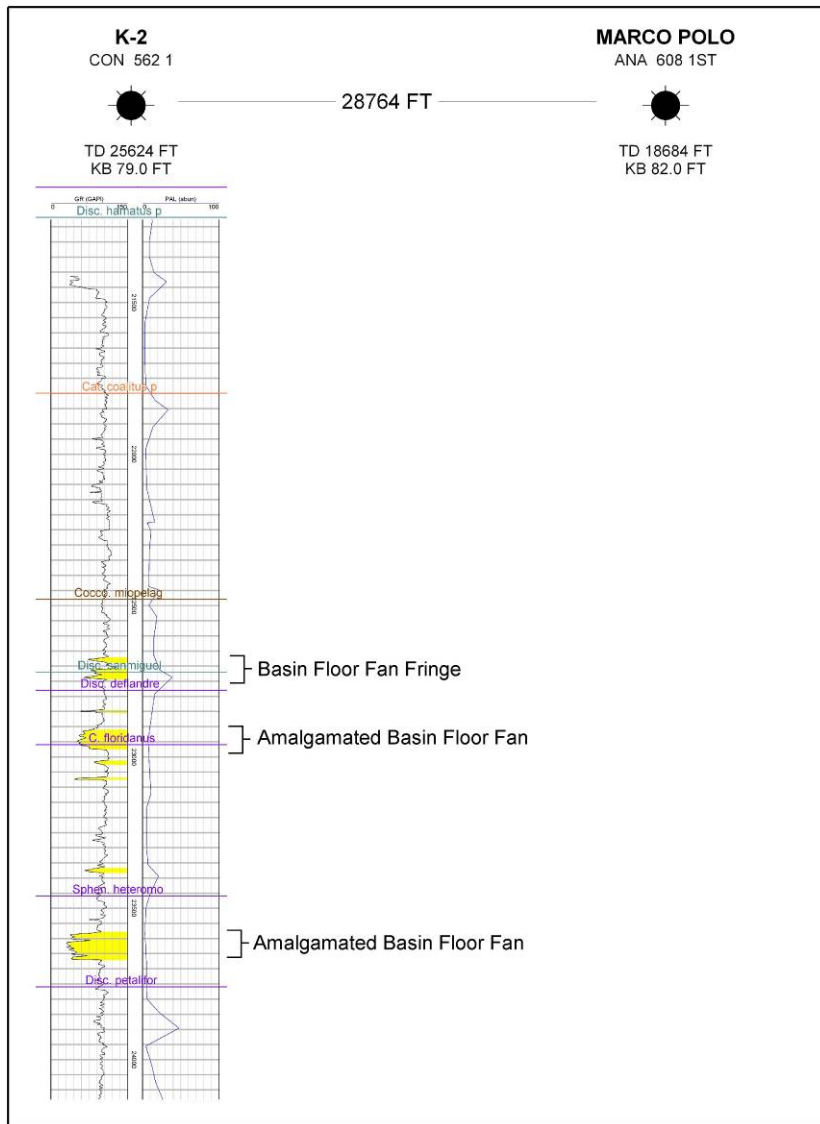
Figure 19—Sand zones color-filled yellow. Thick continuous sands with low gamma responses indicate the presence of basin floor fans.
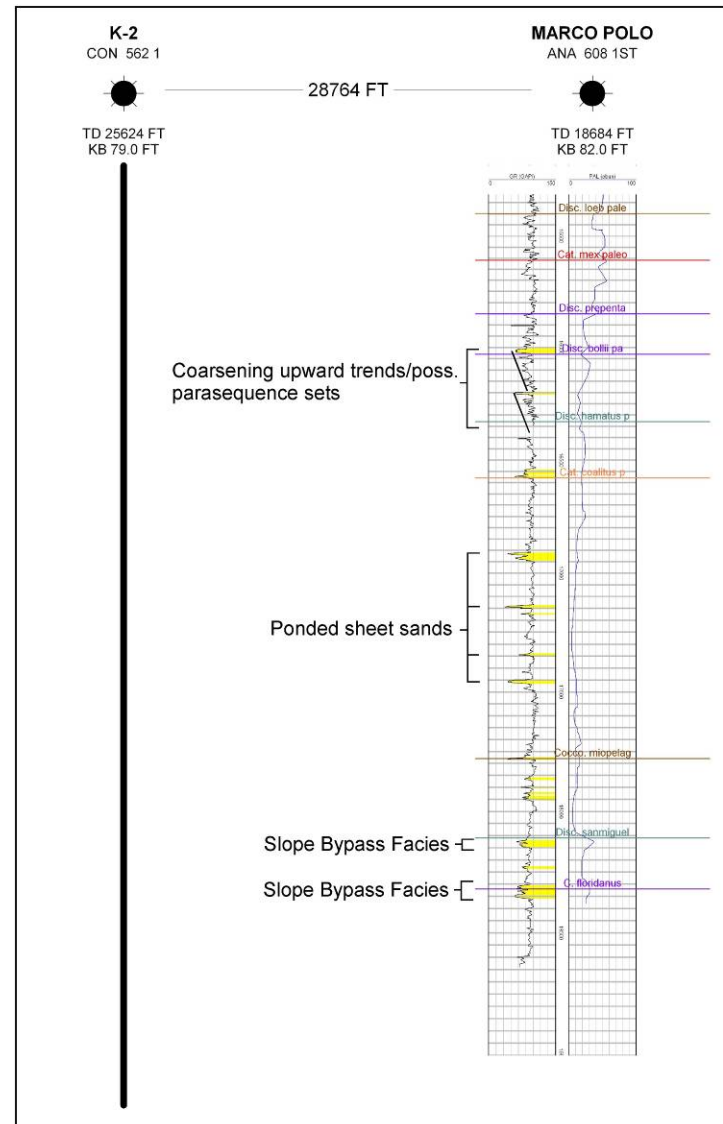
Figure 20—High gamma values indicate possible slope fan and sand-poor slope bypass facies.

39

Study Comparison

Accumulation rates obtained from the maps constructed by Fillon (2005) (Figures 21 through 24) were compared with the observed calculated rates at K-2 and Marco Polo:

Sequence No.	Fillon (2005) Accum. Rate (ft/Ma)	Observed Accum. (ft/Ma)
16	1000-1500 ft/Ma	303
17	1000-1500 ft/Ma	1052
18-20	1800-2500 ft/Ma	712

Table 4—Comparison of Fillon's (2005) predicted accumulation rates versus observed at K-2 (CON 562 #1)

Sequence No.	Fillon (2005) Accum. Rate (ft/Ma)	Observed Accum. (ft/Ma)
16	800-1000 ft/Ma	787
17	600-800 ft/Ma	394
18-20	700-850 ft/Ma	787

Table 5—Comparison of Fillon's (2005) predicted accumulation rates versus observed at Marco Polo (ANA 608 #1ST)

Differences in predicted vs. observed values exist at sequences 16 and 18-20 at K-2, and at sequence 17 at Marco Polo. Theses differences are all within one order of magnitude, but are significant when applied at the exploration scale, as the differences in thickness would represent significant sand thickness changes for a known correlateable reservoir.

It is apparent from the seismic analysis that the minibasin is displaced structurally, and that there is no basis for establishing any consanguinity of stratigraphy between the suprasalt Marco Polo and subsalt K-2 field.
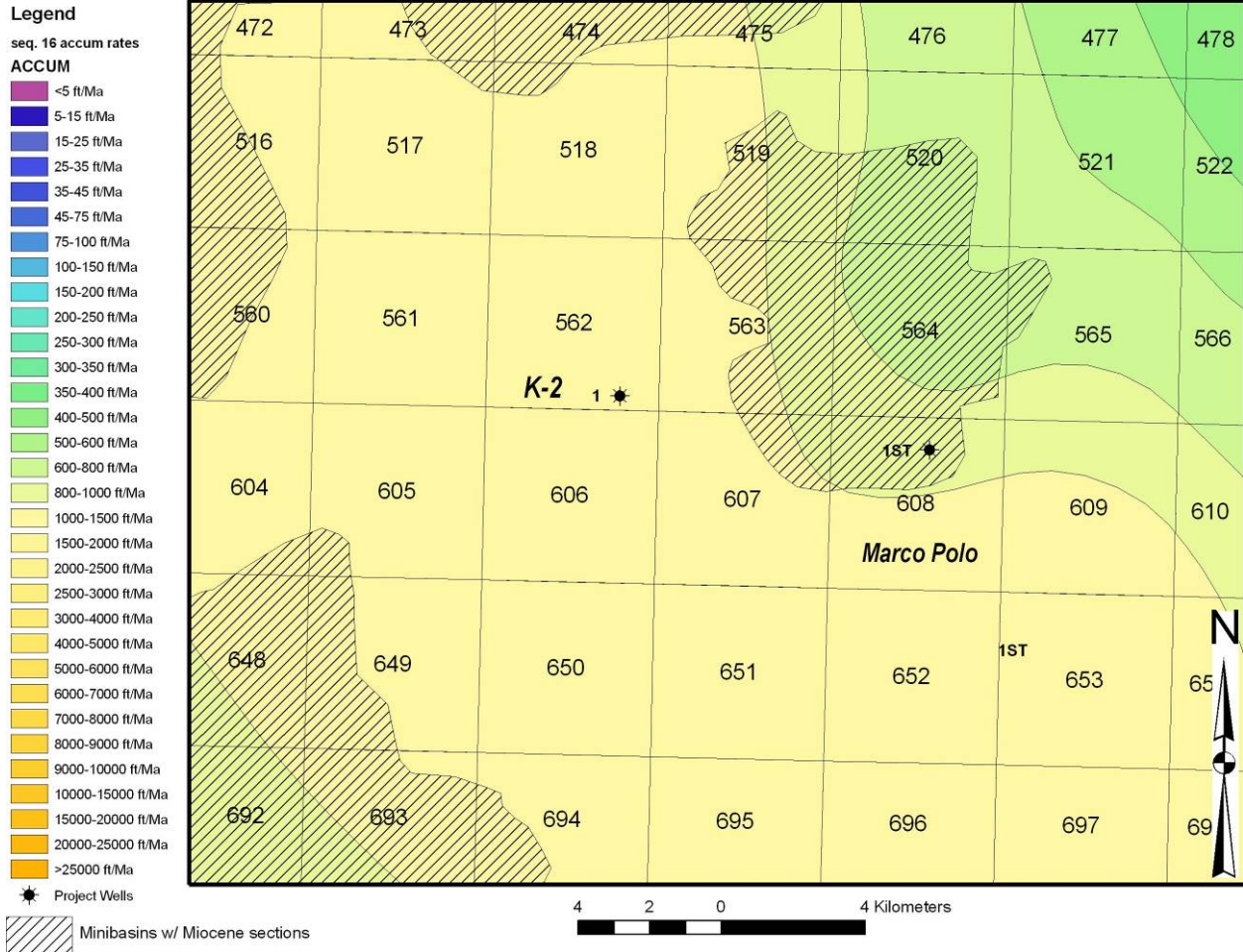
Figure 21—Sequence 16 (9.1-9.4 Ma) accumulation rate map with minibasins shown in cross-hatched areas.
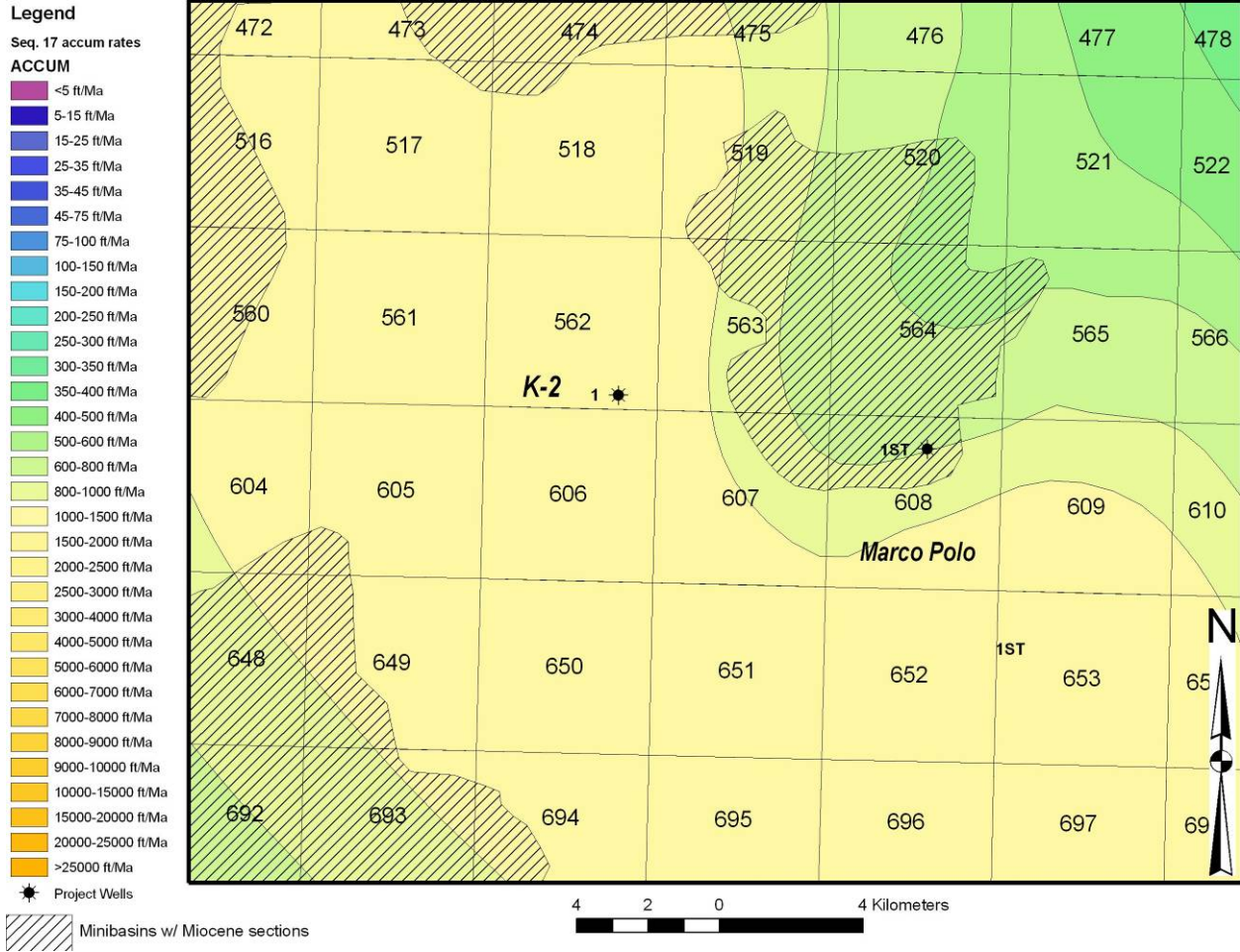
Figure 22—Sequence 17 (9.4-11.0 Ma) accumulation rate map with minibasins shown in cross-hatched areas.
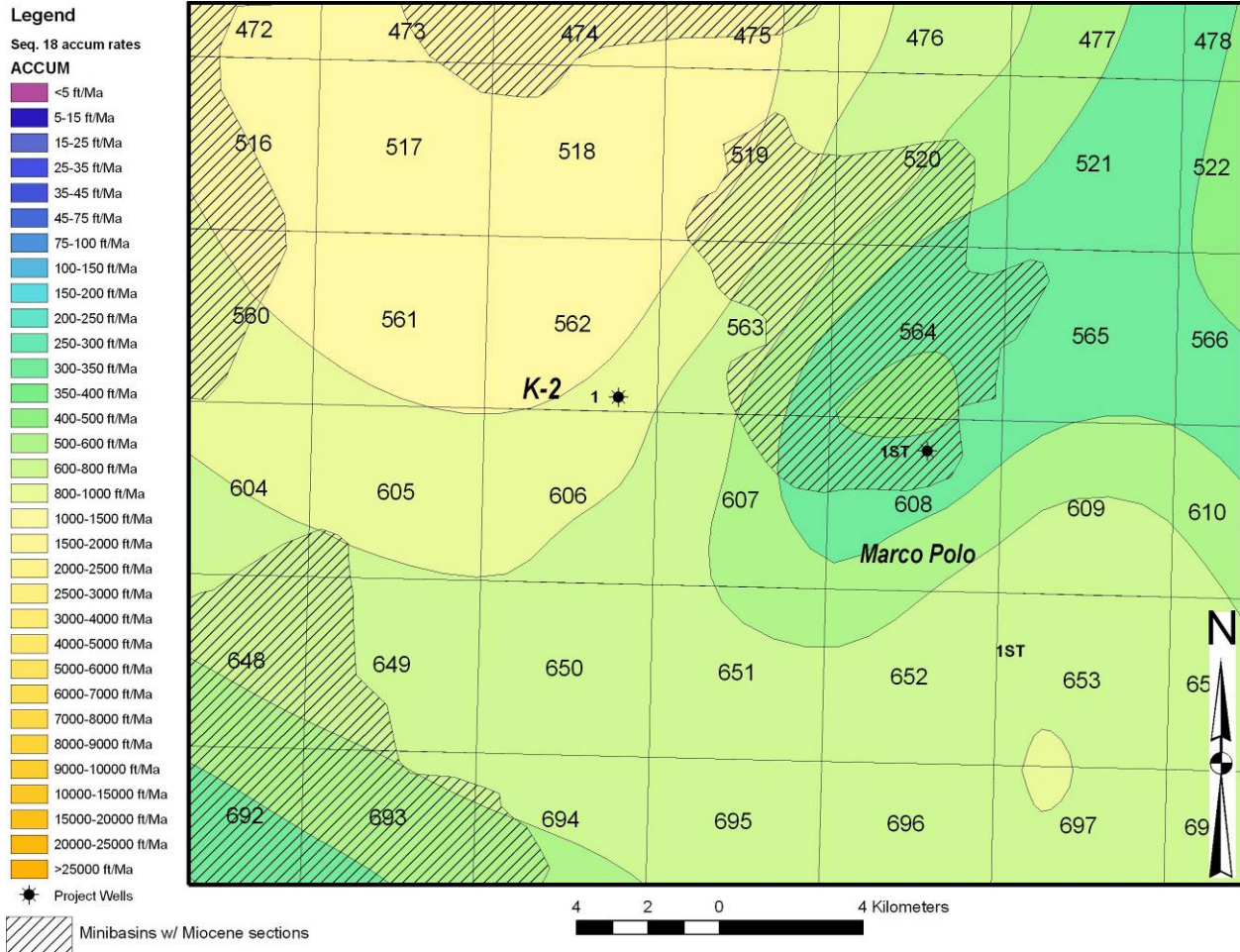
Figure 23—Sequence 18 (11.0-11.9 Ma) accumulation rate map with minibasins shown in cross-hatched areas.
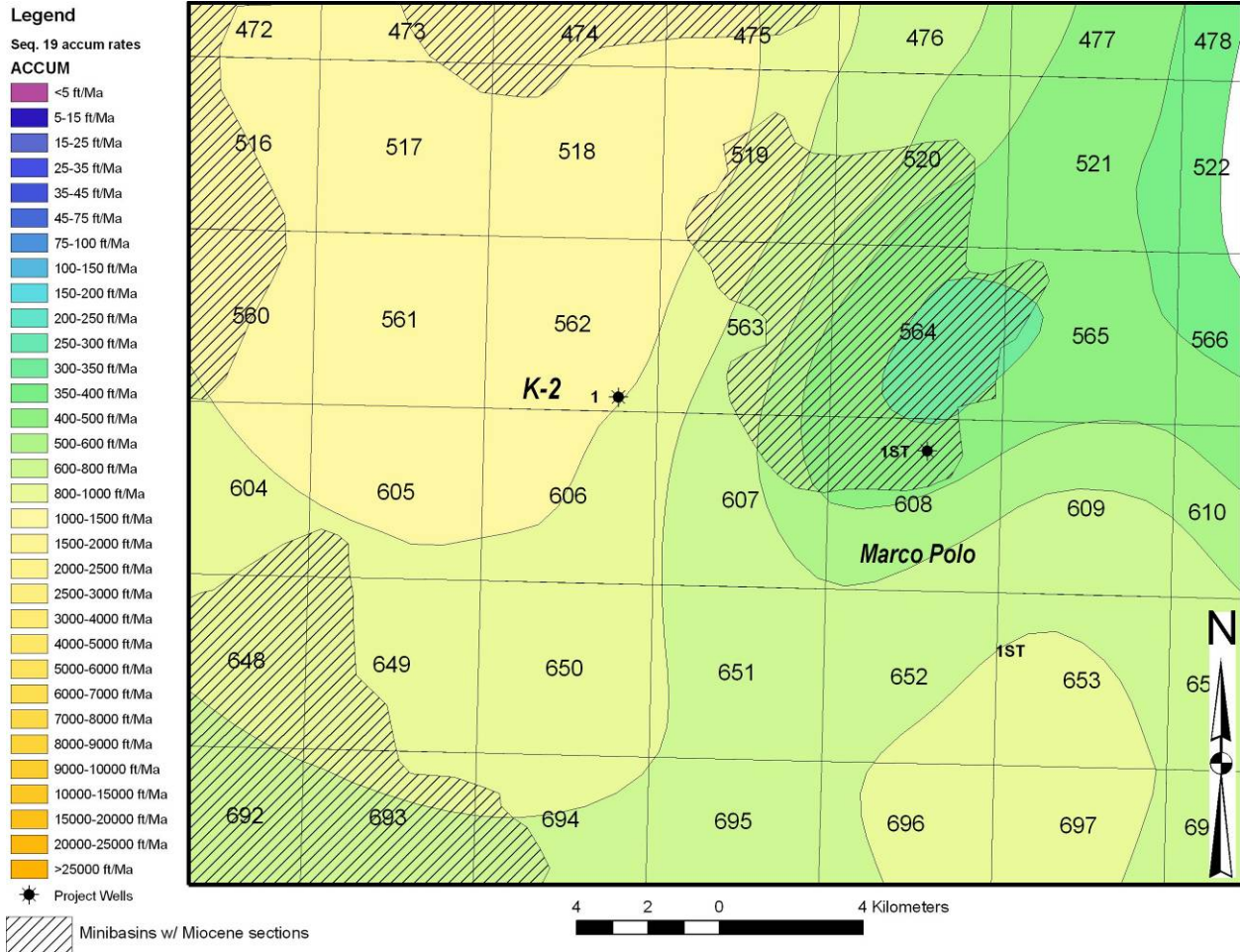
Figure 24—Sequence 19 (11.9-12.8 Ma) accumulation rate map with minibasins shown in cross-hatched areas.

CHAPTER V

DISCUSSION

Implications for Previous Interpretations

The structure and facies analysis presented herein indicates the downslope transport of an entire internally consistent sedimentary section. Rather than this being an isolated exception, gravitational displacement of slope minibasins may be typical in this environment (Rowan et al., 2001). Facies analyses reveal that Middle to Upper Miocene sections within Marco Polo are predominantly slope fan and slope bypass facies. The coeval sections in K-2 are basin floor environments—basin floor fans and pelagic/hemipelagic shales. There is no evidence of continuity between paleo-depositional systems of coeval sections in these fields. Minibasins such as Marco Polo are isolated depo-centers, within which the depositional thicknesses are controlled in large degree to the amount of accommodation space created by salt evacuation. Salt evacuation rates vary over time in the evolution of a minibasin, and each individual basin has a unique tectonic history. Accumulation rate maps from Fillon (2005) assume environmental continuity between control points, which is clearly not the case in the study area due to the isolation of minibasin depocenters (Figs. 21 through 24). This may be an appropriate assumption for the shelf environment, where the basin is generally uninterrupted by salt canopies, and stratigraphic continuity can be laterally extensive. However, his methods are not appropriate in the deep-water slope environment of the Gulf of Mexico for the following reasons:

- Construction of a geostatistical grid does not account for discontinuities such as the isolation of depocenters, or the downslope movement of stratigraphic sections. Reviews of seismic data show many areas where projected sequence intervals may not exist due to

the presence of salt bodies. Gravity induced transport can theoretically place two

biostratigraphically equivalent sections directly on top of each other.

- Autocyclic variability within and between minibasin depocenters yields accumulation

    rates that are not predictable because of the variability of accommodation space induced

    by salt movement. Accumulation rates may be able to be mapped in a true basin floor

    setting, where basin floor fans are aereally extensive and geometrically predictable (Mutti

    and Normark, 1991). Autocyclic variability is the likeliest reason for the observed

    differences between the predicted and actual accumulation rates, especially in the Marco

    Polo field.

Implications for Bio- and Sequence Stratigraphic Models

 The sediment accumulation plots (Figure 7) revealed one potential correlateable

condensed section, however, the comparison of nannofossil abundance curves between the

respective wells revealed no correlateable abundance peaks. Abundance peaks from microfossil

data are an important indicator of condensed sections, as they are often below the scale of

seismic resolution (Armentrout, 1991). A traditional sequence stratigraphic framework predicts

that these condensed sections will be time-synchronous, as they are thought to be primarily

controlled by rising eustatic sea level and reduced sediment input to the deep basin. The results

in this study do not support this prediction, and may be explained by variability in deep-water

deposition. As shown in figure 25, sediment input into the deep basin can have wide lateral

variability. A locus of deposition may exist in relatively close proximity to an area of little

sediment input. Stratigraphic condensation can also occur due to autocyclic controls in

minibasin evolution. In a study that compared oxygen isotope data to fossil abundance, Joyce et

al. (1992) found no consistent relationship between fossil abundance and sea level. The limits of

the resolution of microfossil data from mud returns may also limit the utility of condensed

sections as an exploration tool. Returns are typically sampled at 30 ft intervals. A condensed

interval representing a significant time-span can be much thinner than the sample collection

interval.
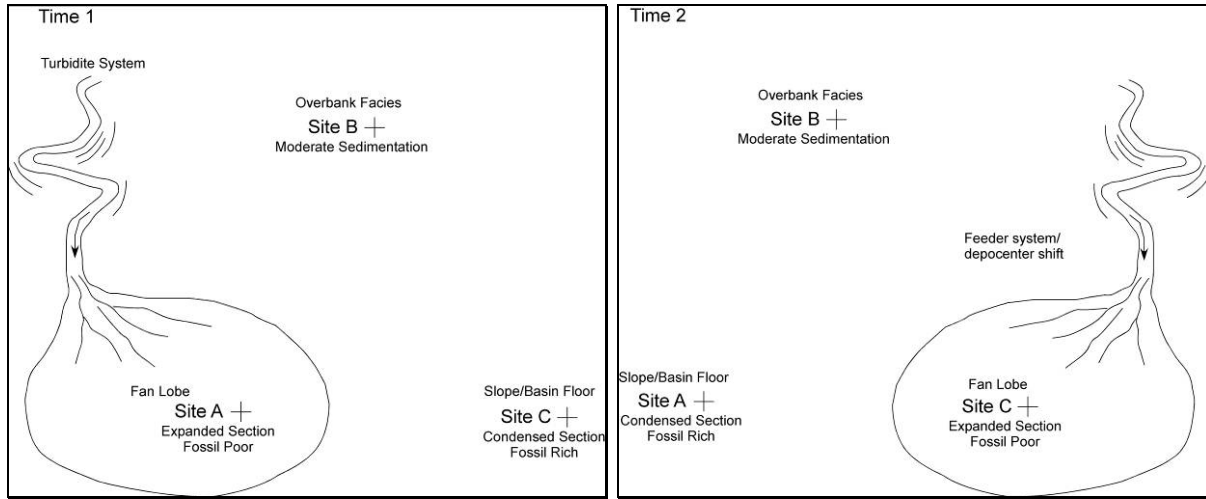
Figure 25—Schematic representation of autocyclic controls on spatial variation of condensed sections. At time 1, site A is experiencing rapid sedimentation, whereas site C is sediment starved. At time 2, the depositional system has shifted; the former location of condensation (site C) is now stratigraphically expanded. Figure contains elements from Joyce et al. (1992).

CHAPTER VI

CONCLUSIONS

The biostratigraphic techniques under review in this study have been widely used on the Gulf of Mexico continental shelf for years with exploration success. Extending their use downslope is a natural progression, but has not always taken the environmental variability of the slope into account. Though biostratigraphy has proven to be a valuable resource in the deep-water, there is a perception by some geoscientists that it is an underutilized tool in this environment (Villamil, 1998). This may be due to the uncertainties of data reliability, and application to this complex environment. Care must certainly be used in any exercise when making regional interpretations from widely spaced control points.

The results of this study have shown that in practice, there is a need for guidelines that should be followed for the proper application of biostratigraphic techniques in the deep-water environment. A practical assessment of biostratigraphic reliability, when used in slope and deep-basin environments world-wide, should include the following:

- Determination of the potential for downslope-rafted allochthonous sections.

- Assessment of variability of and relative dominance of autocyclic and allocyclic controls on basin deposystem activation, especially eustasy and subsidence, when making predictions of deposystem history outside of known control.

- A reduced reliance on the condensed section as a chronostratigraphic surface in the slope and deep basin environments.

Biostratigraphy will likely see increased use, not only as an exploration tool, but also in reservoir development as industry strives to maximize production from known producing fields.

Advances in high-resolution biostratigraphy at the reservoir scale represent the future of new

high-impact applications of this discipline (Giwa et al., 2006).

REFERENCES

Armentrout, J. M., 1991, Paleontologic constraints on depositional modeling: examples of integration of biostratigraphy and seismic stratigraphy, Pliocene-Pleistocene, Gulf of Mexico, *in* P. Weimer and M.H. Link, eds., Seismic facies and sedimentary processes of submarine fans and turbidite systems: New York, Springer-Verlag, p. 137-170.

Brown, A.R., 2004, Interpretation of three-dimensional seismic data, sixth edition: AAPG memoir 42.

Blake, G.H., and A. Gary, 1994, The application of quantitative biostratigraphy of complex tectonic settings, offshore Trinidad, *in* H.L. Lane, G. Blake, and N. McLeod, eds., Graphic correlation and the composite standard: the methods and their applications: Houston, SEPM Research Conference, p. 4.

Bouma, A.H., 2000, Fine grained, mud rich turbidite systems: model and comparison with coarse grained, sand rich systems *in* A.H. Bouma and C.G. Stone eds, Fine grained turbidite systems, AAPG memoir 72, p. 9-20.

Chapin, M.A., P. Davies, J.L. Gibson, and H.S. Pettingill, 1994, Reservoir architecture of turbidite sheet sandstones in laterally extensive outcrops, Ross Formation, Western Ireland, *in* P. Weimer, A.H. Bouma, and B.F. Perkins, eds., Submarine fans and turbidite systems: GCSSEPM 15th Annual Research Conference, p. 53-68.

Chen, Q., Sidney S., 1997, Seismic attribute technology for reservoir forecasting and monitoring: The Leading Edge, v. 16, no. 5, p. 445-509.

Crews, J.R., P. Weimer, A.J. Pulham, and A.S. Waterman, 2000, Integrated approach to condensed section identification in intraslope basins, Plio-Pleistocene, northern Gulf of Mexico: AAPG Bulletin, v. 84, no. 10, p. 1519-1536.

Emery, D. and K.J. Myers, 1996, Sequence Stratigraphy: Oxford, U.K., Blackwell Publishing, 297 p.

Fillon, R.F., and P.N. Lawless, 1999, Paleocene-Lower Miocene sequences in the northern Gulf; progradational slope salt-basin deposition and diminishing slope-bypass deposition in the deep Basin: GCAGS Transactions, v. 49, p. 224 – 241.

Fillon, R.F., and P.N. Lawless, 2000, Lower Miocene-Early Pliocene deposystems in the Gulf of Mexico; regional sequence relationships: GCAGS Transactions, v. 50, p. 411 – 428.

Fillon, R.H., 2003, Multiple overlapping foraminiferal litho-biofacies: applications to deep-water sedimentology and reservoir properties of turbidites: GCAGS Transactions, v. 53, p. 227-242.

Fillon, R.H. 2005. Gulf of Mexico Basin Deposystems – 2005: Comprehensive Well Geohistory Datasets, Chronostratigraphy and Maps: Earth Studies Group, New Orleans, LA. Privately published study.

Giwa, G.O., A.C. Oyede, E.A. Okosun, 2006, Advances in the application of biostratigraphy to petroleum exploration and production: AAPG Search and Discovery art. #50029.

Joyce, J.E., J.M. Prutzman, and L.R.C. Tjalsma, 1992, What is the significance of the condensed interval? Oxygen isotope data from the flexure trend: GCAGS Transactions, v. 42, p. 497-502.

Lawless, P.N., R.H. Fillon, and R.G. Lytton, III, 1997, Gulf of Mexico Cenozoic biostratigraphic, lithostratigraphic, and sequence stratigraphic event chronology: GCAGS Transactions, v. 47, p. 271-282.

Loutit, T.S., J. Hardenbol, P. R. Vail, and G. R. Baum, 1988, Condensed Sections: the key to age dating and correlation of continental margin sequences, *in* C. K. Wilgus, B.S. Hastings, C.G. St. G. Kendall, H.W. Posamentier, C.A. Ross, and J.C. Van Wagoner, eds., Sea level changes: an integrated approach: SEPM Special Publication 42, p. 183-215.

Mann, K.O., and H. R. Lane, eds., 1995, Graphic Correlation: SEPM Special Publication 53, 263 p.

Mitchum, R.M., Jr., P.R. Vail, and J.B. Sangree, 1977, Stratigraphic interpretation of seismic reflection patterns in depositional sequences, *in* C.E. Payton, ed., Seismic stratigraphy— applications to hydrocarbon exploration; AAPG Memoir 26, p. 117-143.

Mitchum, R. M., J. B. Sangree, and P. R. Vail, 1993, Recognizing sequences and systems tracts from well logs, seismic data, and biostratigraphy: Examples from the late Cenozoic of the Gulf of Mexico, *in* P. and H. W. Posamentier, eds., Siliciclastic sequence stratigraphy: Recent developments in applications: AAPG Memoir 58, p. 163-189.

Morris, P.L. and P. Weimer, 2004, Structural geology of the Mississippi Fan fold belt, northern deep Gulf of Mexico, part 2: growth history and evolution: GCAGS Transactions, v. 54, p. 483-503.

Mutti, E., and W.R. Normark, 1991, An integrated approach to the study of turbidite systems, *in* P. Weimer and M.H. Link, eds., Seismic facies and sedimentary processes of submarine fans and turbidite systems: New York, Springer-Verlag, p. 75-106.

Paleo-Data, Inc., Biostratigraphic Chart, Gulf of Mexico, Neogene. Ver. 0410, A.S. Waterman.

Pirmez, C., R.T. Beubouef, S.J. Friedmann, and D.C. Mohrig, 2000, Equilibrium profile and base level in submarine channels: examples from Late Pleistocene systems and implications for the architecture of deep-water reservoirs, *in* P. Weimer, R.M. Slatt, J. Coleman, N.C. Rosen, H. Nelson, A.H. Bouma, M.J. Styzen, and D.T. Lawrence, eds., Deep-water reservoirs of the world: GCSSEPM Foundation 20th Annual Research Conference, p. 782-805.

Prather, B.E., J.R. Booth, G.S. Steffens, and P.A. Craig, 1998, Classification, lithologic calibration, and stratigraphic succession of seismic facies of intraslope basins, deep-water Gulf of Mexico: AAPG Bulletin, v. 82, no. 5A, p. 701-728.

Reading, H.G., M. Richards, 1994, Turbidite systems in deep-water basin margins classified by grain size and feeder system: AAPG Bulletin, v. 78, no. 5, p. 792-822.

Rowan, M.G., B.C. Vendeville, and F.J. Peel, 2001, The role of salt in gravitational failure of passive margins, *in* R.H. Fillon, N.C. Rosen, P. Weimer, A. Lowrie, H. Pettingill, R.L. Phair, H.H. Roberts, and B. van Hoorn, eds., Petroleum systems of deep-water basins: GCSSEPM Foundation 21st Annual Research Conference, p. 221-228.

Shaffer, B.L., 1990, The nature and significance of condensed sections in Gulf Coast Late Neogene sequence stratigraphy: GCAGS Transactions, v. 40, p. 767-776.

Shaw, A.B., 1964, Time in stratigraphy: New York, McGraw-Hill Book Co., 365 p.

Slatt, R.M., 2006, Petroleum geology of deepwater (turbidite) depositional systems: AAPG short course notes.

Villamil, T., C. Arango, P. Weimer, A. Waterman, M.G. Rowan, P. Varnai, A.J. Pulham, and J.R. Crews, 1998, Biostratigraphic techniques for analyzing benthic biofacies, stratigraphic condensation, and key surface identification, Pliocene and Pleistocene sediments, northern Green Canyon and Ewing Bank (offshore Louisiana), northern Gulf of Mexico: AAPG Bulletin, v. 82, no. 5B, p. 961-985.

Vail, P.R., R.G. Todd, and J.B. Sangree, 1977, Chronostratigraphic significance of seismic reflections, *in* C.E. Payton, ed., Seismic stratigraphy—applications to hydrocarbon exploration; AAPG Memoir 26, p. 99-116.

Waltham, D., and I. Davison, 2001, Obstacle and sinks: effects of turbidite flow on deepwater continental margins, *in* R.H. Fillon, N.C. Rosen, P. Weimer, A. Lowrie, H. Pettingill, R.L. Phair, H.H. Roberts, and B. van Hoorn, eds., Petroleum systems of deep-water basins: GCSSEPM Foundation 21st Annual Research Conference, p. 511-522.

Weimer, P., P. Varnai, F.M. Budhijanto, Z.M. Acosta, R.E. Martinez, A.F. Navarro, M.G. Rowan, B.C. McBride, T. Villamil, C. Arango, J.R. Crews, and A.J. Pulham, 1998, Sequence stratigraphy of Pliocene and Pleistocene turbidite systems, northern Green Canyon and Ewing Bank (offshore Louisiana), northern Gulf of Mexico: AAPG Bulletin, v. 82, no. 5B, p. 918-960.

APPENDIX

WesternGeco

July 14, 2006

Mr. David Wade
Murphy Exploration & Production Company
131 South Robertson Street
New Orleans, LA 70161

REFERENCE: Permission to use Seismic Data

Dear Mr. Wade:

WesternGeco is pleased to authorize Murphy Exploration & Production Company's request to provide data licensed from WesternGeco's Green Canyon survey (Data) to an intern, (Andrew Tipton) in Murphy's UNO Student Internship Program. Murphy has provided this Data to Mr. Tipton for use in his thesis.

As WesternGeco standard policy, this Data will be utilized solely for research in support of Mr. Tipton's thesis and related publications. It is additionally understood that:

1. Mr. Tipton acknowledges that this Data constitutes a valuable trade secret of WesternGeco and agrees not to show, divulge, sell, lend or otherwise disclose the Data to anyone except as may be authorized in writing by WesternGeco and Murphy.

2. It is agreed that the Data is to be utilized solely for the purpose of completing the thesis. Use of the Data for any other purpose will be allowed only if WesternGeco agrees in writing to such use of the Data.

3. Publications should indicate that the Data is provided courtesy of WesternGeco and should describe the location of the Data in a general manner, deleting specific geographical references. The scale of such visual representations will not exceed 8.5" x 11".

Once again, we are pleased to assist your intern, Andrew Tipton, in pursuit of his educational endeavor. Please acknowledge acceptance of these terms on Murphy's behalf by signing and returning one original to me at the address on the letterhead. Additionally, please have your intern sign the document as well.

55

Mr. David Wade
Murphy Exploration & Production Company
Page 2

REFERENCE: Permission to use Seismic Data

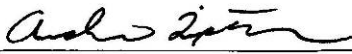If you have any questions or comments, please feel free to contact me at 713-689-1063.

Sincerely,

Debbie Jez
Contracts Administrator, MultiClient Data Sales

cc: Andrew Tipton

Agreed and Accepted - Murphy Exploration & Production Company

Name: _____

Title: Sr. Geophysicist

Date: 1 August 2006

Agreed and Accepted - Andrew Tipton

Name: _____

Date: 21 Aug 2006

56

VITA

Andrew Tipton was born in Hampton, Virginia and received his B.S. from the University of Florida in 2000. He was a geoscientist at Foster Wheeler Environmental in Stuart, Florida from 2001 to 2002, where he performed environmental assessment and remediation studies. After working in Stuart, he moved to Gainesville, Florida where he worked in the field of Karst subsidence at Geohazards, Inc., until enrolling at the University of New Orleans. He has accepted a geoscience position with Chesapeake Energy Corporation in Oklahoma City, where he will reside upon graduation.